1-1-2008

Integrated Late Quaternary chronostratigraphy for San Salvador Island, Bahamas: Patterns and trends of morphological change in the land snail Cerion

Paul Hearty
University of Wollongong, paulh@uow.edu.au

Stephen A. Schellenberg
San Diego State University

Integrated Late Quaternary chronostratigraphy for San Salvador Island, Bahamas: Patterns and trends of morphological change in the land snail Cerion

Abstract

Reconstructing the phylogeny and biogeography of the Caribbean land snail *Cerion* requires a robust stratigraphic and chronological framework. To this end, we have determined the stratigraphic succession on San Salvador, a Bahamian island with a rich fossil and modern *Cerion* fauna. A primary purpose of this paper is to independently verify this succession through whole-rock and *Cerion* aminostratigraphies and AMS ^{14}C-based age models. Over 150 individual *Cerion* shells were age-ranked from 140 ka to modern using stratigraphic position and reverse-phase HPLC (RPC) amino acid racemization, which was sufficiently sensitive to resolve stratigraphic subunits within the Holocene and late Pleistocene. A secondary purpose of this paper is to assess broad changes in the gross morphology (height, width) of supersets of *Cerion* from age-ranked lots spanning this ~ 140 kyr chronostratigraphy. Through each of the three interglacial sequences (i.e., marine isotope stages 5e, 5a, and 1), between-sample trends in mean gross morphology often greatly exceed within-sample variances (± 1σ). Live-collected *Cerion* exhibit a range in gross morphology that nearly encompasses that of the entire fossil sequence. A trend of increasing gross shell size characterizes each of the interglacial phases, with a major step-decrease between marine isotope stages 5a and 1. While between-unit variation is often great in *Cerion* from SSI, within-unit variation appears unimodal through the record.

Keywords

Integrated, Late, Quaternary, chronostratigraphy, for, San, Salvador, Island, Bahamas, Patterns, trends, morphological, change, land, snail, Cerion

Disciplines

Life Sciences | Physical Sciences and Mathematics | Social and Behavioral Sciences

Publication Details

Hearty, P. and Schellenberg, S. A. (2008). Integrated Late Quaternary chronostratigraphy for San Salvador Island, Bahamas: Patterns and trends of morphological change in the land snail Cerion. Palaeogeography, Palaeoclimatology, Palaeoecology, 267 41-58.

Integrated Late Quaternary chronostratigraphy for San Salvador Island, Bahamas: Patterns and trends of morphological change in the land snail *Cerion*

Paul J. Hearty [a,*], Stephen A. Schellenberg [b]

[a] GeoQuest Research Centre, School of Earth and Environmental Sciences, University of Wollongong, Wollongong NSW, 2522 Australia
[b] Department of Geological Sciences, San Diego State University, 5500 Campanile Drive, San Diego, CA 92182-1020 USA

ARTICLE INFO

Article history:
Received 9 August 2007
Received in revised form 16 May 2008
Accepted 5 June 2008

Keywords:
The Bahamas
San Salvador Islands
Cerion land snails
Biostratigraphy
Amino acid racemization
Reverse-phase high-performance liquid chromatography
Accelerator mass spectrometry ^{14}C chronology

ABSTRACT

Reconstructing the phylogeny and biogeography of the Caribbean land snail *Cerion* requires a robust stratigraphic and chronological framework. To this end, we have determined the stratigraphic succession on San Salvador, a Bahamian island with a rich fossil and modern *Cerion* fauna. A primary purpose of this paper is to independently verify this succession through whole-rock and *Cerion* aminostratigraphies and AMS ^{14}C-based age models. Over 150 individual *Cerion* shells were age-ranked from 140 ka to modern using stratigraphic position and reverse-phase HPLC (RPC) amino acid racemization, which was sufficiently sensitive to resolve stratigraphic subunits within the Holocene and late Pleistocene. A secondary purpose of this paper is to assess broad changes in the gross morphology (height, width) of supersets of *Cerion* from age-ranked lots spanning this ~140 kyr chronostratigraphy. Through each of the three interglacial sequences (i.e., marine isotope stages 5e, 5a, and 1), between-sample trends in mean gross morphology often greatly exceed within-sample variances ($\pm 1\sigma$). Live-collected *Cerion* exhibit a range in gross morphology that nearly encompasses that of the entire fossil sequence. A trend of increasing gross shell size characterizes each of the interglacial phases, with a major step-decrease between marine isotope stages 5a and 1. While between-unit variation is often great in *Cerion* from SSI, within-unit variation appears unimodal through the record.

1. Introduction

Despite a high diversity of named living taxa (i.e., over 600 named species; see website: http://invertebrates.si.edu/Cerion/species_list.cfm), relatively few investigations have examined the Caribbean pulmonate land snail *Cerion* from a paleontological perspective (Dall, 1905; Mayr and Rosen, 1956; Gould and Woodruff, 1978; Woodruff and Gould, 1980; Gould and Woodruff, 1986; Gould, 1988; Goodfriend and Gould, 1996). Such a perspective can provide a broader biological context and important constraints on the rates and directions of morphological change and, by extension, the evolutionary history of this pervasive and readily preserved constituent of terrestrial island ecosystems. *Cerion* land snails are widespread throughout the Florida Keys, Bahamas, Greater Antilles, Cayman Islands, western Virgin Islands, Dutch Antilles, but are absent in Jamaica, the Lesser Antilles, and coastal Central and South America (Pilsbry, 1902; Maynard, 1913; Clench, 1957). The large number of named species and subspecies presents a daunting challenge to even the most skilled systematist, and begs the fundamental question of 'what constitutes a species'? Perspectives and approaches to this question may range from modern genetic studies within a biogeographic framework to fossil morphologic studies within a chronostratigraphic framework.

San Salvador Island (Figs. 1 and 2) in the Bahamas has been subject to an intense and diverse range of scientific research, largely due to the infrastructure support provided through the Gerace Research Centre (formerly Bahamian Field Station). Challenges facing earlier investigations in discerning the lithostratigraphy involved the discontinuous, disjunct, and relatively monotonous petrographic nature (i.e., relatively pure limestone) of the deposits. Progress has been made in unravelling the stratigraphic succession (Carew and Mylroie, 1985, 1987), particularly with the aid of whole-rock aminostratigraphy (Hearty and Kindler, 1993; Hearty and Kaufman, 2000; in review). These advances in the geologic realm now encourage progress in the area of invertebrate paleontology and biostratigraphy, particularly with regard to the land snail *Cerion* (Rose, 1989, Hearty et al., 1993, Walker and Hearty, 1993, Walker, 1994, Gould, 1997). Several paleontological papers on *Cerion* have been published on other islands (Garrett and Gould, 1984; Gould and Woodruff, 1986; Goodfriend and Gould, 1996), but are limited by examining only a few isolated time-intervals without rigorous age control.

Like the overall stratigraphic picture of the Bahamas (Kindler and Hearty, 1996; Hearty and Kaufman, 2000), the lithologic succession on SSI consists of couplets of interglacial marine and eolian carbonate facies and glacial-age paleosol facies dating back to probably marine

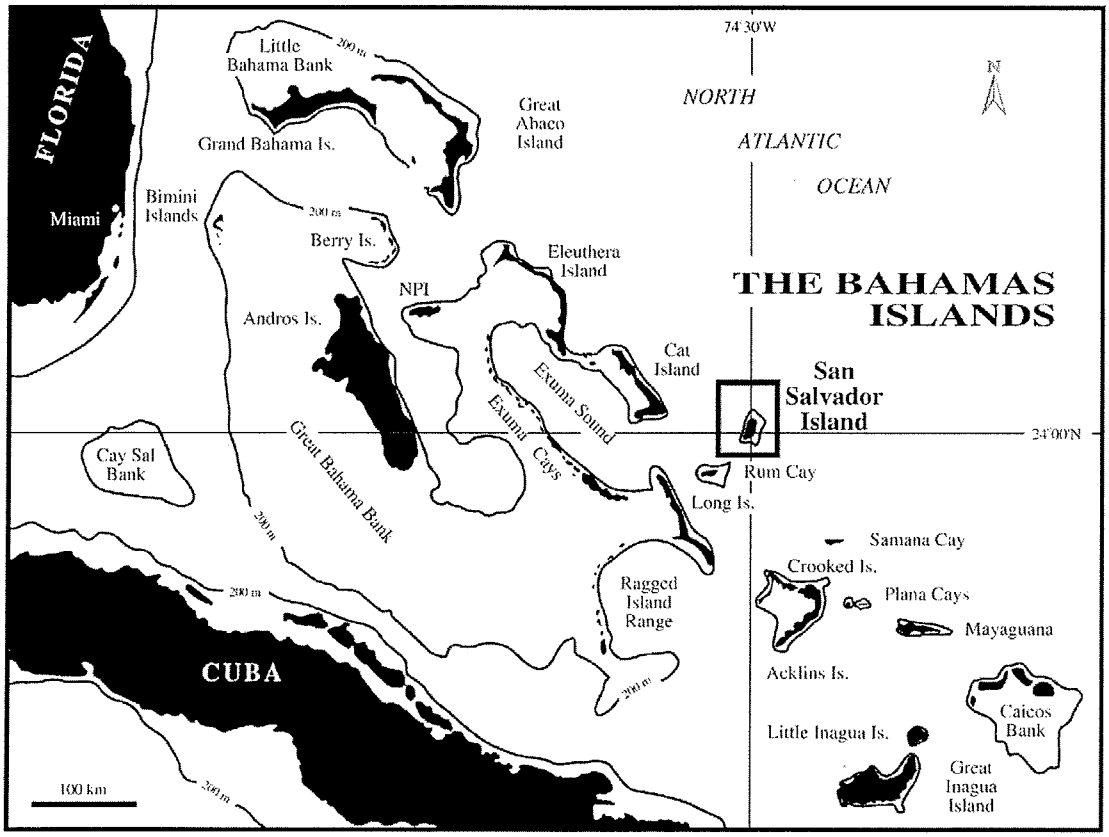

Fig. 1. Map of the Bahamas showing many of the 700 rocks and islands distributed across Great and Little Bahama Banks. Like numerous smaller limestone pinnacles of the Bahamas, San Salvador Island is isolated from the larger Banks even during the lowest lowstands.

isotope stage (MIS) 13 or 15 (Fig. 2). Within the eolianite carbonate facies are weak interglacial soils or "protosols" (defined in Vacher and Hearty, 1989), which were colonized by plants and animals during pauses in eolianite deposition. These protocols often contain assemblages of plant rhizomorphs, *Cerion*, and land-crab fossils (i.e., *Gecarcinus ruricola* and *Cardisoma guanhumi*, with the former a primary predator on *Cerion* (Quensen and Woodruff, 1997)). During sufficiently high sea levels (i.e., MIS 5e, 5a, and 1), the partial to near complete flooding of the SSI platform resulted in voluminous production of bioclastic- and ooid-dominated sands that progressively built up the island from shoals to beach and coastal dune facies. During lower sea levels (i.e., weaker interglacials through glacial extremes), the subaerial exposure of the SSI platform fostered the weathering of exposed interglacial carbonates and the accumulation of atmospheric dust, which together promoted the development of brown to red clayey paleosols. For this study, fossils and rocks from the three youngest highstand cycles are investigated, corresponding with MIS 5e, 5a and/or 5c, and 1.

1.1. Specific aims and objectives

The objectives of this study are: (1) to rank the relative ages of fossil and living *Cerion* populations, and their associated lithologic sample units, based on stratigraphic succession and amino acid ratios of whole-rock and *Cerion* samples; (2) to establish a relative-age time series comprising D/L ratios from *Cerion* and to apply existing age models calibrated with radiometric ages to stratigraphic successions; and (3) to assess gross morphological trends and patterns in *Cerion* within and among the Pleistocene, Holocene, and modern populations.

1.2. Changes in paleobiogeography of Cerion

Glacial and interglacial sea-level fluctuations resulted in significant spatial changes in the physical geography of the entire Bahamian region. For example, a 10 to 20 m fall of modern sea level would transform nearly 700 islands of the Bahamas (Fig. 1: Great Bahama Bank: Andros, New Providence, Eleuthera, Cat, Exumas, Long, Acklins, Crooked, etc. and Little Bahama Bank: Grand Bahama and Abaco) into major landmasses of sub-continental proportions. During highstands, the Bahama platforms were flooded to varying degrees, creating chains of islands from higher hilltops and forcing terrestrial ecosystems to spatially constrict to these smaller refugia. *Cerion* was continously under pressure from major ecological and environmental transformations associated with these massive ecological events of repeated isolation and unification of these Grand Bahama Bank and Little Bahama Bank islands.

In contrast, SSI (Figs. 1 and 2) is one of several smaller Bahamian islands that would have remained oceanographically isolated during even the lowest Pleistocene sea levels associated with the most extreme glacial intervals. Thus, unlike the terrestrial biotas of the Great Bahama Bank, SSI would have been subjected to relatively small changes in land area (<30%), and *Cerion* would have evolved in relative isolation. Considering its remote oceanic setting and the reduced opportunities for landfall of *Cerion* from other sources, presumably climate change and predation pressures would be the primary evolutionary forces affecting the land snail. Thus, in many ways, SSI may be considered as a microcosm for exploring and understanding the natural history of *Cerion*.

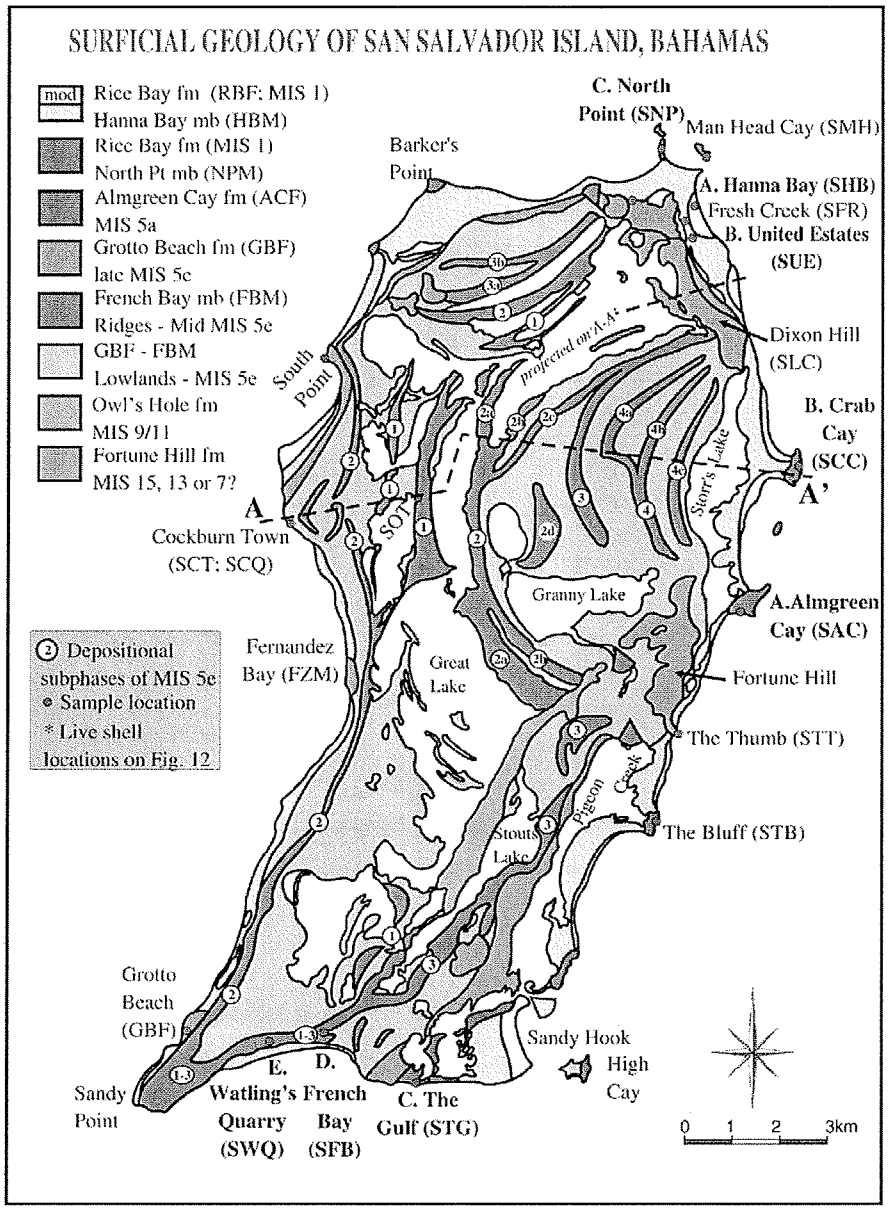

Fig. 2. Geological map of SSI (modified from Hearty and Kindler, 1993) showing areal distribution of formations, correlation with MIS, the *A–A'* cross-section shown in Fig. 3, and key study locations mentioned in the text. Sites from Figs. 7 and 8 are labelled in bold. Names in the legend are explained in Table 1.

1.3. Stratigraphic framework of SSI

The stratigraphic framework of SSI includes middle and late Pleistocene limestones and soils as well as a succession of Holocene units (Table 1 and Figs. 2 and 3). The middle Pleistocene Owl's Hole and Fortune Hill Formations are correlated with two or more interglacial stages between MIS 15 and 9/7. Grotto Beach, Almgreen Cay, and Rice Bay Formations are correlated with MIS 5e, 5a, and mid to late MIS 1, respectively (Hearty and Kindler, 1993; Hearty and Kaufman, 2000) (Fig. 2). Table 1 correlates these established SSI lithostratigraphic units with marine isotope stages (MIS) as well as other lithostratigraphic units from other regions.

In living forms, *Cerion* on SSI exist in greatest numbers within a few hundred meters of the coastline in palmetto scrub and sea grape communities on both windward and leeward sides of coastal dunes. As fossils, nearly all *Cerion* on SSI are found in weak brown or tan protosols developed upon, or on the leeward margin of, interglacial eolian or mixed eolian-marine facies (Hearty et al., 1993). *Cerion* are also common within interbedded complex brown and reddish soils and micrite lenses and within calcrete capping interglacial units, which may temporally extend to the onset of glacial intervals. *Cerion* shells are rarely found in good condition in glacial-age red to brown paleosols, even in the stratigraphically youngest intervals. This distribution reflects some combination of diagenesis (e.g., shallow subsurface dissolution and leaching within glacial-age soils), ecology (e.g., decreased absolute abundance; biogeographic tracking of maritime microclimates), and taphonomy (e.g., increased surface exposure, crab use and predation, and thereby increase physical and biotic degradation due to decreased sedimentation rates). As a result, the best available SSI collection of fossil *Cerion* consists primarily of collections from MIS 6/5e, 5e/5d, 5c–5a/4 transitions, and multiple phases within MIS 1, with very sparse populations from MIS 4-2

Table 1
Nomenclature and correlation of major units on SSI with major stratigraphic units in Bahamas and Bermuda and isotope stages and substages

Period	San Salvador (Carew and Mylroie, 1985; 1995)	San Salvador (Hearty and Kindler, 1993)	The Bahamas (Hearty and Kaufman, 2000)	Bermuda (Hearty et al., 1992; Hearty, 2002)	Marine isotope Stage (MIS)
Holocene (10 to 0 ka)	Hanna Bay Mb, RBF	East Bay Mb, RBF	Couplet Vib	Recent	Late 1
		Hanna Bay Mb, RBF	Couplet Vib		Mid 1
	North Point Mb, RBF	North Point Mb, RBF	Couplet Via		Mid 1
Glacial palaeosol	----------	----------	----------	----------	2,3,4
Late Pleistocene	Unrecognized	Almgreen Cay Fm	Couplet V	Southampton Fm	5a
(135 to 75 ka)	Unrecognized	Man Head Cay		Hungry Bay Fm	5c?
	Weak palaeosol	----------	----------	----------	5d
	Unrecognized	Fernandez Bay Mb, GBF	Couplet Ivc	Devonshire Bay Mb, RBF	Late 5e
	Cockburntown Mb, GBF	Cockburntown Mb, GBF	Couplet Ivb		5e
	French Bay Mb, GBF	French Bay Mb, GBF	Couplet Iva	Grape Bay Mb, RBF	5e
Glacial palaeosol	----------	----------	----------	----------	6/8
Middle Pleistocene	Unrecognized	Fortune Hill Fm	Couplet III	Upper Town Hill Fm	7/9*
(500 to 200 ka)	Glacial palaeosol	----------	----------	----------	8/10
	Owl's Hole Fm	Owl's Hole FM	Couplet II	Lower Town Hill Fm	9/11
	Unrecognized	Unrecognized	Couplet II		9/11
	Unrecognized	Unrecognized	Couplet I	Base of Goulding Cay (Hearty, 1998)	≥137

Correlation with Bermuda's stratigraphy is offered for comparison. RBF=Rice Bay Fm; GBF=Grotto Beach Fm; RBF=Rocky Bay Fm (see Carew and Mylroie, 1987; Hearty and Kindler, 1993, 1994 for details). *We now believe that outcrops forming the core of both Fortune Hill and Dixon Hill Fms are older than the Owl's Hole Fm, and perhaps formed during MIS 13 or 15.

(70–10 ka). While major field efforts were made to collect *Cerion* from a broad geographic and stratigraphic coverage, the distribution of geological formations and their outcrops (Fig. 2) naturally introduced some unavoidable spatial sampling bias. Further complicating an unbiased fossil survey is the impenetrable scrub, highly-indurated bedrock, and watery interior of the island. Sample sites in this study are listed in Table 2 and shown in Fig. 1.

2. Materials and methods

2.1. Field methods

Cerion-bearing soils vary considerably in thickness from 0.5 to >3.0 m. In the thicker units, up to four stratigraphic levels were collected, and in some cases the uppermost collected levels were only <0.2–0.5 m below the upper contact or surface, which tends to expose the samples to greater thermal and other diagenetic effects than deeper samples. Regardless of these less than optimal parameters for amino acid racemization (AAR) geochronology, such samples were analysed in order to directly quantify the extent of these surface-related effects.

Sections were stratigraphically logged, photographed, and plotted on 1:25,000 topographic maps. Shell and rock samples were collected and bagged with date, field number, sample composition, and apparent stratigraphic context (i.e., formation, member, and subunit). Sample "Field #" for all sites and tables in this work are explained as follows using SHB3x(2) as an example: "S"=San Salvador Island; "HB"=Hanna Bay site (see Table 2 for all locality codes); "3"=third collection from HB site; "x"=stratigraphic position of collected unit at HB3, where "a" is oldest and "z" is the youngest; "(2)"=second sub-collection up from base

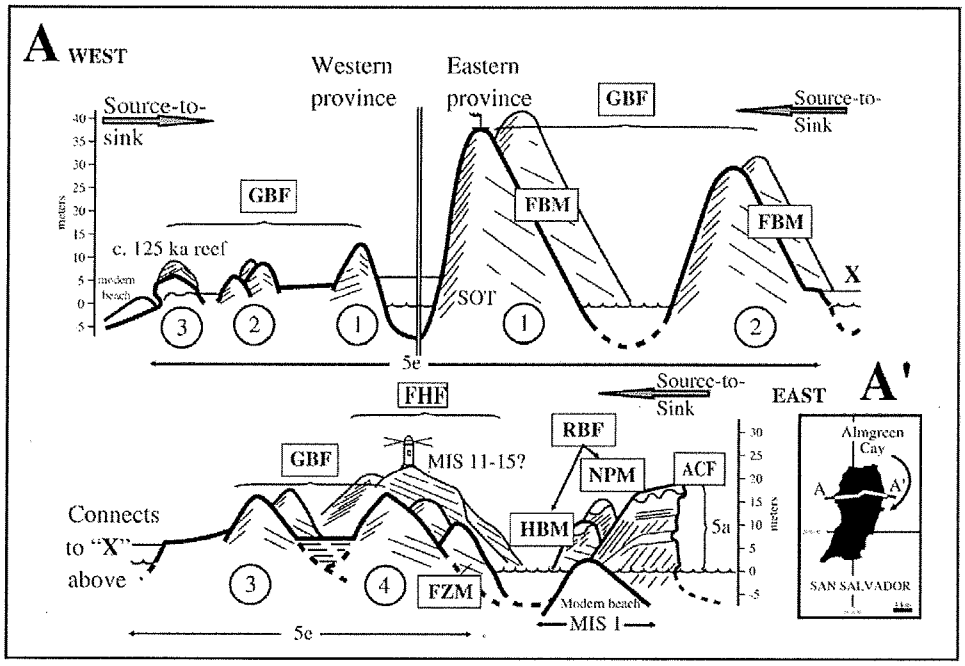

Fig. 3. Morphostratigraphic succession on SSI (modified after Hearty and Kindler, 1993). Abbreviations as follows: RBF=Rice Bay Formation (North Point (NPM) and Hanna Bay Members (HBM)); ACF=Almgreen Cay Formation; GBF=Grotto Beach Formation (French Bay (FBM) and Fernandez Bay Members (FZM).

Table 2
Summary of sample ranking, field numbers, apparent correlation with stratigraphic units and MIS (see Fig. 1), D/L and radiometric or estimated ages

Rank	Field #	Marine isotope stage	*Cerion* measured *N*	D/L Asp (unit mean±1σ)	D/L Glu (unit mean±1σ)	AAR shells analysed *N*	AMS ^{14}C cal BP known (yr), or estimated age (ka)
Live-collected shells							
3	SMH1z	1	25				
4	SCC3z	1	18	0.103±0.006	0.040±0.005	3	2 yr
5	SNP6z	1	26				
6	SNP7z	1	20				
7	SHB3z	1	11	0.034±0.005	0.016±0.001	3	2 yr
8	STT1z	1	23				
9	SSH2z	1	26				
10	SSH1z	1	25				
11	SWQ1z	1	19				
12	SGB1z	1	22				
13	SSU1z	1	11				
14	SVH1z	1	25				
15	SBR1z	1	27				
Surface dead shells							
16	SMH1-s	1	4				
17	SFR1x	1	11	0.266±0.010	0.171±0.011	3	
18	SCC1z	1	12	0.103±0.006	0.040±0.005	3	602±50 cal BP
19	SCC1-s	1	6				
20	SMH1g(z)	1	8				
21	SAC1-s	1	10				
22	SAC6z	1	5				
23	SNP1-s	1	10				
24	SHT1z	1	18	0.237±0.019	0.061±0.004	3	865±67 cal BP
25	SBB1-s	1	–				
26	SBB2z(1)-s	1	2				
Late MIS 1 (East Bay Mb or unnamed)							
27	STD1d-s	1	30				
28	STD1b-s	1	–				
29	STD2b.1-s	1	1				
30	SNP3d-s	1	21				
31	SNP5c(3)	1	9	0.385±0.041	0.151±0.033	5	
Mid MIS 1 (Rice Bay Fm (RBF) — North Point and Hanna Bay Mbs)							
32	SUE1x(4)	1	12	0.429±0.026	0.177±0.025	5	
33	SHB3x(3)	1	14	0.449±0.083	0.225±0.113	3	
34	SHB3f-s	1	10				
35	SHB3x(2)	1	20	0.457±0.040	0.193±0.033	6	
36	SUE1x(3)	1	20	0.503±0.032	0.231±0.015	5	
37	SUE1x(2)	1	18	0.517±0.018	0.209±0.009	5	
38	SUE1x(1)	1	12	0.498±0.033	0.194±0.015	5	3971±93 cal BP
39	SNP5c(2)	1	13	0.476±0.056	0.204±0.048	7	
40	SNP3c-s	1	17				
41	SHB3x(1)	1	2	0.450±0.036	0.199±0.024	2	5583±79 cal BP
42	SHB1x mid	1	2	0.480±0.003	0.206±0.008	2	
43	SNP5c(1)	1	23	0.539±0.081	0.279±0.046	7	6351±46 cal BP
44	SNP5-s	1	22				
MIS 4 to 2 (glacial soils)							
45	SCC4e-s	1–4	9				
46	SAC1g(2)	1–4	6	0.511±0.013	0.242±0.028	3	
47	SAC1g-s	1–4	2				
48	STB1e-s	5a/4	7				50–70
Early to late MIS 5a (Almgreen Cay Fm — ACF)							
49	SCC3d(4)	5a	9	0.750±0.020	0.641±0.024	3	70–80
50	SCC4d(3)	5a	8	0.744±0.035	0.635±0.051	4	70–80
51	SCC4d(1–2)	5a	16	0.727±0.036	0.616±0.034	7	70–80
52	SCC4d-s	5a	14				70–80
53	SCC4b.5-s	5a	10				70–80
54	SCC4b.3-s	5a	9				70–80
55	SCC4b.1-s	5a	12				70–80
56	SAC2c	5a	5	0.797±0.040	0.658±0.035	5	80–90
57	SAC2b-s	5a	8				80–90
58	SAC2b	5a	9	0.759±0.058	0.600±0.043	7	80–90
59	SAC2aa	5a	8	0.760±0.017	0.624±0.050	4	80–90
60	SCC6aa-s	5a	3				80–90
61	STB1b-s	5a	4				80–90
62	STG1c(3)	5a	12	0.687±0.042	0.653±0.057	3	80–90
63	STG1d-s	5a	18				80–90
64	STG1c(2)	5a	30	0.749±0.051	0.665±0.066	4	80–90
65	STG1c(1)	5a	16	0.703±0.071	0.629±0.072	7	80–90
66	STG1b-s	5a	–				80–90

(continued on next page)

Table 2 (*continued*)

Rank	Field #	Marine isotope stage	*Cerion* measured *N*	D/L Asp (unit mean±1σ)	D/L Glu (unit mean±1σ)	AAR shells analysed *N*	AMS ^{14}C cal BP known (yr), or estimated age (ka)
Late MIS 5e/5c? Uncertain older or younger stratigraphic correlation							
67	SMH2e.2-s	5c?	12				90–110
68	SMH1b	5c?	17	0.731±0.048	0.664±0.046	6	90–110
69	SMH1e.1-s	5c?	7				90–110
70	SSP2c-s	5c/5e	0				110–120
71	SWQ2d(2)	5c/5e	9	0.652±0.045	0.643±0.047	3	110–120
Early to late MIS 5e (Grotto Beach Fm: GBF)							
72	SWQ1d(1)	5e	14	0.745±0.046	0.684±0.044	6	115–125
73	SWQ2d(1)	5e	5	0.800±0.021	0.758±0.010	3	115–125
74	SWQ1d.3-s	5e	4				115–125
75	SWQ1d.2-s	5e	10				115–125
76	SWQ1d.1-s	5e	19				115–125
77	SWQ1cc-s	5e	1				115–125
78	SWQ1c-s	5e	4				115–125
79	SWQ1c(1)	5e	7	0.789±0.033	0.734±0.012	5	115–125
80	SFB4e-s	5e	9				115–125
81	SFB4d/5d-s	5e	7				115–125
82	SFB5d-s	5e	–				115–125
83	SFB5b-s	5e	6				115–125
84	SFB4b-s	5e	12				125–140
85	SFB4b(1)	5e	16	0.782±0.034	0.734±0.029	7	125–140
86	SOT3a-s	5e	2				125–140

Stratigraphic rank ("Rank") is determined by 1) physical stratigraphic superposition (if known); 2) D/L Glu; 3) then D/L Asp. Ranking does not apply to live and surface dead collections whose numbers are used for identification and tracking only.

of HB3x. All subsequent dashed-codes (e.g., "-s") are collection trip identifiers.

Simple linear measurements (Fig. 4) of maximum height (*H*; parallel to axis of coiling), maximum width (*W*; perpendicular to axis of coiling), aspect ratio (*H*/*W*), and total size (*H*+*W*) were made on a total of 986 shells from 70 fossil and 13 live collections. The purpose of this simple morphometric approach is to document general changes in size and shape through the biostratigraphic succession. It is not intended to define taxonomic or phylogenetic characteristics; indeed, we avoid discussion of species names in this investigation. General qualitative observations of shell ornamentation and coloration were made on previous collections from the same units in Hearty et al. (1993). About half of the sample levels, representing all known stratigraphic units less than 140 ka, were analyzed for AAR.

2.2. AMS ^{14}C ages and atmospheric and marine reservoir effects

Both the whole-rock sediment and *Cerion* shells were sonicated repeatedly until the water was clean, and then leached 30% by dry weight and rinsed numerous times with DDI water. The dry sample submitted for AMS dating consisted of ~50 mg of solid grains without cements. Because dune sediments are composed of ooids or the skeletons of marine organisms formed in shallow waters on the shelf, a marine reservoir age (Stuiver et al., 2005) was applied to all AMS ^{14}C ages from sediments. Representative subsets were selected for ^{14}C analyses on the basis of D-alloisoleucine/L-isoleucine (or A/I) on whole-rock samples and D/L aspartic (Asp) and glutamic acid (Glu) data on *Cerion* land snails.

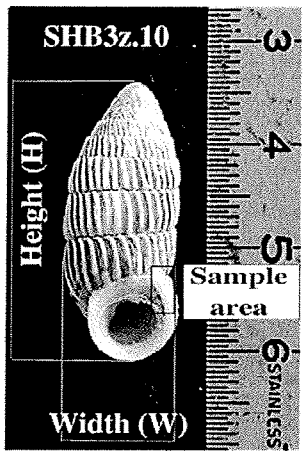

Fig. 4. Image showing location of extracted RPC samples from modern and fossil *Cerion* shells, along with height (*H*) and width (*W*) morphometric measures.

We chose the standard reservoir age (ΔR=0) because, although the evidence from the region is sparse, the available ages are not significantly different from 400 yr (calib.qub.ac.uk/marine/index). All ^{14}C ages were calibrated to calendar years before 1950 AD (cal BP) using CALIB 5.0 (Reimer et al., 2004; Stuiver et al., 2005). We used the median of the probability distribution of the calibrated ages. All ages are reported in cal BP with errors of one-half of the one-sigma calibrated age range.

2.2.1. A "dead carbon" correction of AMS ^{14}C ages?

Land snails that graze or estivate on limestone substrates can incorporate older carbon (by ingestion or absorption) into their shells. Previous studies indicate that *Cerion* have a highly variable "dead carbon" anomaly. Goodfriend and Stipp (1983) and Goodfriend and Gould (1996) determined dead carbon anomalies of 740, 810, and 1520 yr from three live-collected, pre-bomb *Cerion* from the Margach Cay, Anguilla Cay, and Inagua, Bahamas. To further assess the dead carbon effect, we analysed additional specimens of known age from museum collections (Hearty and Kaufman in review). Unfortunately, essential contextual details for the historical samples, such as the exact location and probable age of the substrate at the collection sites were rarely recorded, or known, by the collector. In theory, higher age anomalies would be expected if the snails lived and grazed on older "carbon dead" Pleistocene limestone. Much lower anomalies would be predicted if the snails lived on limestone terrane formed only a short time before colonization by the snails.

For the ^{14}C results in this study and Hearty and Kaufman (in review), we have established that the difference in ages between dune-sediment formation and colonizing snails is generally small (±1000 yr), suggesting that the potential for incorporation of a

significant amount older or dead carbon is limited. Our analyses from SSI support this view. For example, a *Cerion* shell from Crab Cay on SSI (i.e., SCC1z), collected dead on the surface of a late Holocene dune, has an Asp D/L value of 0.099, and a calibrated ^{14}C age of 610±50 cal BP (Table 1). Although the D/L value could be somewhat elevated by heating of surface shells, making the age appear older based on the Asp D/L values of other live-collected shells (Hearty and Kaufman in review), the ratio of 0.099 equates to a maximum age of about 220 yr. Subtracting this value yields an anomaly of 390 yr. Comparisons with mean AAR ages generated from our age model presented below further support this view, and provide a useful methodology for evaluating the reliability of ^{14}C ages on land snails.

From these and previous experiments, we conclude that, without abundant pre-bomb specimens collected from substrates of known age, quantifying the dead carbon anomaly is unrealistic. Furthermore, carbon acquisition from modern vegetation versus ancient carbonate sediments may also vary considerably among individuals, depending on their life habits and on local climate, and thus the magnitude of the anomaly is inherently unpredictable. If a correction were applied, it would be a constant value (as in Goodfriend and Gould, 1996), with little effect on the relative ages, age differences, or rates of change.

2.3. Amino acid racemization (AAR) geochronology: past and present

The AAR method depends on progressive decomposition of proteins and amino acids preserved in fossil material. The measured A/I or D/L Asp and Glu values serve as an index of the relative age of the organism. The underlying theory and various applications of the AAR method are summarized in Rutter and Blackwell (1995). Initial forays into SSI AAR determinations (Hearty et al., 1993; Hearty and Kindler, 1993) employed different instruments and preparations, such as sample desalting with hydrofluoric acid, following Hare and Mitterer (1967). This earlier preparation method, using ion-exchange (IE) high-performance liquid-chromatography (HPLC), discriminated the same clusters or modal classes of A/I ratios (or "aminozones"; Hearty et al., 1986), but produced systematically higher values (~10%; Hearty and Kindler, 1993) relative to those produced by the more recent techniques described below.

AAR studies in the Bahamas (e.g., Hearty and Kindler, 1993, 1994; Kindler and Hearty, 1996) used improved IE techniques (without HF desalting) according to protocols in Miller and Brigham-Grette (1989) to determine the extent of *epimerization* of A/I on primarily whole-rock samples (Hearty et al., 1992).

In this study, we augment published whole-rock data for SSI with new data obtained by the more recently developed "reverse-phase" HPLC (RPC) technique (Kaufman and Manley, 1998), which facilitates fast, efficient, and economic analyses. RPC provides similar accuracy and greater precision compared to IE, and requires substantially less carbonate material (i.e. <0.1 mg for RPC versus >10 mg for IE), which reduces damage to fossils and allows for subsequent specimen analyses such as AMS ^{14}C, stable isotopes, and morphometrics. In this study, RPC analyses provide D/L *racemization* products for four amino acids (aspartic (Asp), glutamic (Glu), serine (Ser), and alanine (Ala)). Comparative rates between the IE and and RPC methods were assessed by split-analyses of a subset of *Cerion* samples in Hearty and Kaufman (in review). A/I ratios for whole-rock samples were determined using the standardized laboratory IE methods, procedures, and protocols of Kaufman at Utah State University and Northern Arizona University (Miller and Brigham-Grette, 1989; Hearty and Kaufman, in review). We stress that each analytical methods is used for a different purpose: IE A/I (Ile epimerisation) is the standard for whole-rock samples from host rocks, while RPC racemisation of Asp and Glu D/L are used primarily for *Cerion* shells; together these methods produce independent but parallel aminostratigraphic records.

2.4. Sample preparation and analysis

2.4.1. IE-HPLC whole-rock samples

Preparation procedures for whole-rock samples are outlined in Hearty (1998). The standard grain-size range for whole-rock samples (Hearty et al., 1992; Hearty and Kaufman, 2000) has traditionally been 250–850 μm. However, whole-rock samples were dominated by 250–425 μm grains, and therefore exclusively this grain-size was used. Two replicate subsamples were prepared and analyzed from each numbered sample. Preparation involved repeated hand-milling, screening through a 850–425–250 μm sieve stack until all sturdy grains were separated and cements entirely removed, followed by brief sonication, and a weak hydrochloric acid treatment to remove the outermost ~10% mass of the carbonate grains. Solutions were flushed with N_2, sealed in sterile vials, hydrolyzed at 110°C for 22 h, then dried in a vacuum desiccator. After rehydration, samples were injected onto an IE that employs post-column derivatization in *O*-phthaldialdehyde (OPA) and fluorescence detection. Each sample solution was analyzed two to three times and the results averaged, producing an analytical precision of peak-height A/I ratios of typically <3%.

Table 3
Summary of whole-rock A/I data compared with major and minor stratigraphic subdivisions from SSI

AA lab #	Field #	Locality [^{14}C cal BP]	Comp	MIS	A/I	±1σ
Holocene — recent (cf. Rice Bay Fm)						
5152 A	SFR 1x	Fresh Pond	Sk	Late 1	0.120	0.002
1262A	SHB2b	Hanna Bay Mb	Sk	mid 1	0.091	0.004
5155 A	SHB3x	Hanna Bay Mb [4601±80]	Sk	mid 1	0.111	0.005
5154 A	SUE1x	United Estates [5161±92]	Sk	mid 1	0.091	0.001
1263A	SNP4a	North Point Mb	Oo	mid 1	0.079	0.004
5156 A	SNP5a	North Point Mb [5996±68]	Oo	mid 1	0.096	0.001
Latest Late Pleistocene (cf. Almgreen Cay Fm)						
5146 A	SCC4a	Crab Cay	Sk	5a	0.324	0.008
1264A	SAC1c	Almgreen Cay Fm	Sk	5a	0.377	0.007
5157 A	SAC2b	Almgreen Cay Fm	Sk	5a	0.355	0.002
1264B	SAC2a	Almgreen Cay Fm	Sk	5a	0.348	0.002
1569A	SAC2a	Almgreen Cay Fm	Sk	5a	0.377	0.001
5147 A	STG2e	The Gulf	Sk	5a?	0.398	0.009
5153 A	SMH1b	Man Head Cay	Sk	5c?	0.262	0.013
Late Pleistocene (cf. Grotto Beach Fm)						
1096A	SFB4a	French Bay Mb	Oo	5e	0.399	0.003
1096B	SFB4c	French Bay Mb	Oo	5e	0.415	0.004
1096D	=1096A	French Bay Mb	Oo	5e	0.405	0.014
1096C	SOT3b	French Bay Mb	Oo	5e	0.370	0.001
1267A	SOT1b	Observation Tower Rd	Oo	5e	0.476	0.009
1267B	SOT1c	Observation Tower Rd	Oo	5e	0.448	0.009
1098A	SKBZ1	Cockburntown Mb	Oo	5e	0.431	0.002
1570A	STG1e	The Gulf	Sk	5e	0.376	0.003
5149 A	SFB4a	French Bay Mb	Oo	5e	0.356	0.001
5149 A	SFB4a	French Bay Mb	Oo	5e	0.361	0.005
1571A	SWQ1c	Watlings Quarry	Oo	5e	0.379	0.003
5148 A	SWQ1c(2)	Watlings Quarry	Oo	5e	0.344	0.005
1572A	SCQ1aa	C-Town Quarry	Oo	5e	0.324	0.006
1266A	SCTB1	Cockburntown reef	Sk/Oo	5e	0.292	0.004
1266B	SCTD1c	Cockburntown reef	Sk/Oo	5e	0.332	0.005
1265A	SFS1a	Field Station	Oo/pel	5e	0.351	0.014
Middle Pleistocene (cf. Dixon Hill and Owl's Hole Fms (Table 1)						
1269A	SLC4	Lighthouse Cave	Sk/pel	7/13	0.368*	0.016
1270A	SWQ1a	Watlings Quarry	Sk	9/11	0.698	0.007
1268A	STT1	The Thumb	Sk	>13	0.426*	0.021

Not included are whole-rock data from Hearty and Kindler (1993), prepared under a different protocol, which yielded the same aminostratigraphic subdivisions, but produced systematically higher A/Is than in subsequent preparations. Type members (Mb) and formations (Fm) are identified in column 3 along with AMS ^{14}C ages (Table 4) from sediment samples. Each A/I ratio and 1σ error represents the analysis of 2 subsamples from the same sediment collection.
*Samples are depleted in amino acids, yielding unreliable values.

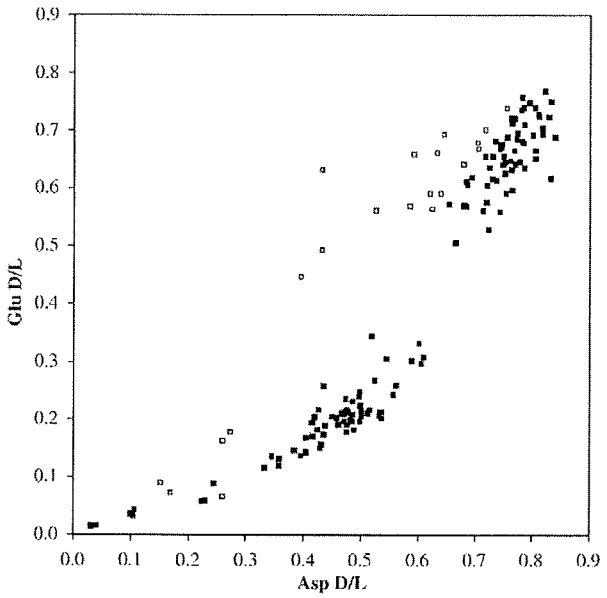

Fig. 5. Covariate plot of all D/L Asp and Glu data from 150 *Cerion* shell samples from SSI. The boundary between Holocene and Pleistocene is indicated by a gap in D/L Glu values between approximately 0.35 to 0.50.

2.4.2. Cerion preparations and reverse-phase (RPC) analysis

RPC analytical protocols followed those for ostracodes (Kaufman and Manley, 1998; Kaufman, 2003), foraminifera (Hearty et al., 2004), and ooids (Hearty et al., 2006). Adult *Cerion* are easily recognized by reverse coiling and enlargement of the apertural lip, and only such adult shells were analysed. A total of 150 *Cerion* shells were analysed by RPC from San Salvador. Every shell was routinely sampled from the same location of the apertural lip, where a small fragment (~1–5 mg) was removed with a sterile nail clipper near the suture between the last whorl and the lip. Samples were weighed, leached of 10–30% of their mass, and rinsed repeatedly with ultrapure water. Samples were air-dried under laminar flow, reweighed into 100 µl conical micro-reaction vials, dissolved using the same formulation as for WR samples, hydrolized for 6 h at 110 °C, and dried in a vacuum desiccator. Prior to RPC analysis, samples were rehydrated with slightly acidified DDI water containing a 0.01 mM L-*h*Arg spike adjusted to sample weight.

The RPC procedure employs pre-column derivatization with OPA together with the chiral thiol, *N*-isobutyryl-L-cysteine, to yield fluorescent diastereomeric derivatives of chiral primary amino acids. The derivatization was performed on-line prior to each injection using an auto-injector. Separation was by a reverse phase column packed with a C_{18} stationary phase (Hypersil BDS, 5 µm) using a linear gradient of aqueous sodium acetate, methanol, and acetonitrile (for details see Kaufman and Manley, 1998). Detection was by fluorescence. Chemstation computer software integrated the fluorescence signal based on peak area and controlled the eluent gradient and automated sample derivatization and injection program. A 60-minute RPC analysis yields D/Ls of Asp, Glu, Serine (Ser), L-*h*Arg (internal standard), and alanine (Ala), but only Asp and Glu are used for geochronological determinations. These amino acids are among the most abundant in *Cerion* and are the best analytically resolved.

2.4.3. An age model for Cerion from the Central Bahamas and San Salvador Island (Hearty and Kaufman in review)

Rather than develop age equations for each island or group of islands, we combine our entire RPC and AMS ^{14}C data sets (23 ^{14}C ages and 507 D/L analyses for *Cerion* from the central Bahama Islands to yield a rigorously supported age model (Hearty and Kaufman in review). The rate of racemization for Glu and Asp in *Cerion* over the last 7 ka was calibrated using paired ^{14}C and AAR analyses from the same shell, combined with D/L data from shells collected live up to 112 yr ago. We used least-squares regression to fit the D/L values and their corresponding ^{14}C ages and collection dates to derived empirical age equations. The y-intercept of the regression lines were fixed such that the mean D/L values of living shells collected in 2005 intercepted a date of −55 calendar years BP in order to correct all ages to the ^{14}C chronology, where $t=0$ at 1950. To constrain the rate of racemization over the initial phases of the reaction, we incorporated the mean D/L values and associated known ages for the eight collections of live-collected shells from the Bahamas, Cuba, and Florida. In the context of the last 7000 yr as determined from ^{14}C ages, we suggest that these shells accurately reflect the rate of racemization in fossil shells from the Bahamas.

The rate of racemization for Asp under constant temperature follows an exponential function (e.g., Kaufman, 2006). By raising Asp

Table 4
Results of AMS ^{14}C analyses of carbonate sediment and *Cerion* shell samples from San Salvador Island

U of AZ ID #	Sample name (UAL)	$\delta^{13}C$ (‰)[a]	Reported ^{14}C age (yr BP)	±1σ	Cal BP	±1σ
Sediment samples [sk=skeletal; oo=oolitic]						
AA69287	[sk] SUE1x (5154A)	0	4860	53	5161	92
AA69288	[oo] SNP5a (5156A)	2.8	5602	47	5996	68
AA69289	[sk] SHB3x (5155A)	1.4	4429	43	4601	80
Cerion land snail samples						
AA69298	SHT1z (5091C)	−6.0	973	43	865	67
AA69299	SCC1z (5187B)	−4.9	642	37	602	50
AA69300	SUE1x(1) (5099C)	−4.3	3648	53	3971	93
AA69301	SNP5c(1) (5102D)	−0.6	5558	40	6351	46
AA69302	SHB3x (5093E)	−5.7	4838	47	5583	79

AAR ages calculated from *Cerion* D/L Asp and Glu are available in Appendix A.
[a] $\delta^{13}C$ values = 0 are assumed.

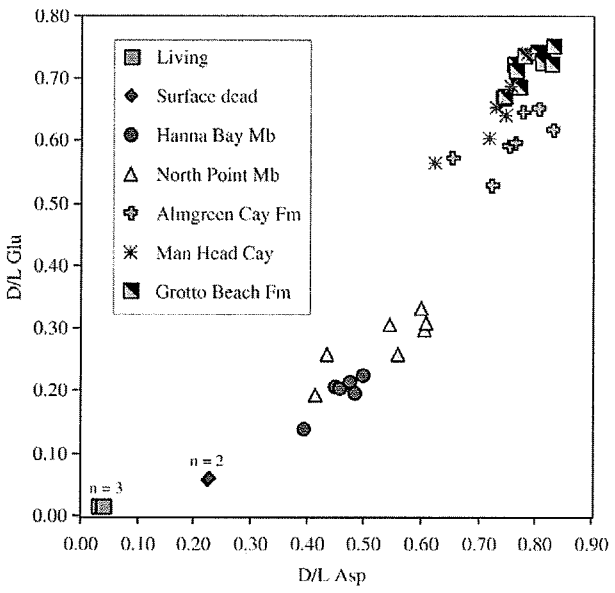

Fig. 6. Covariate plot of D/L Asp and Glu values from the type localities of major stratigraphic units on SSI. All major formations and members are distinguished, while some sites such as The Gulf yield an intermediate range of values.

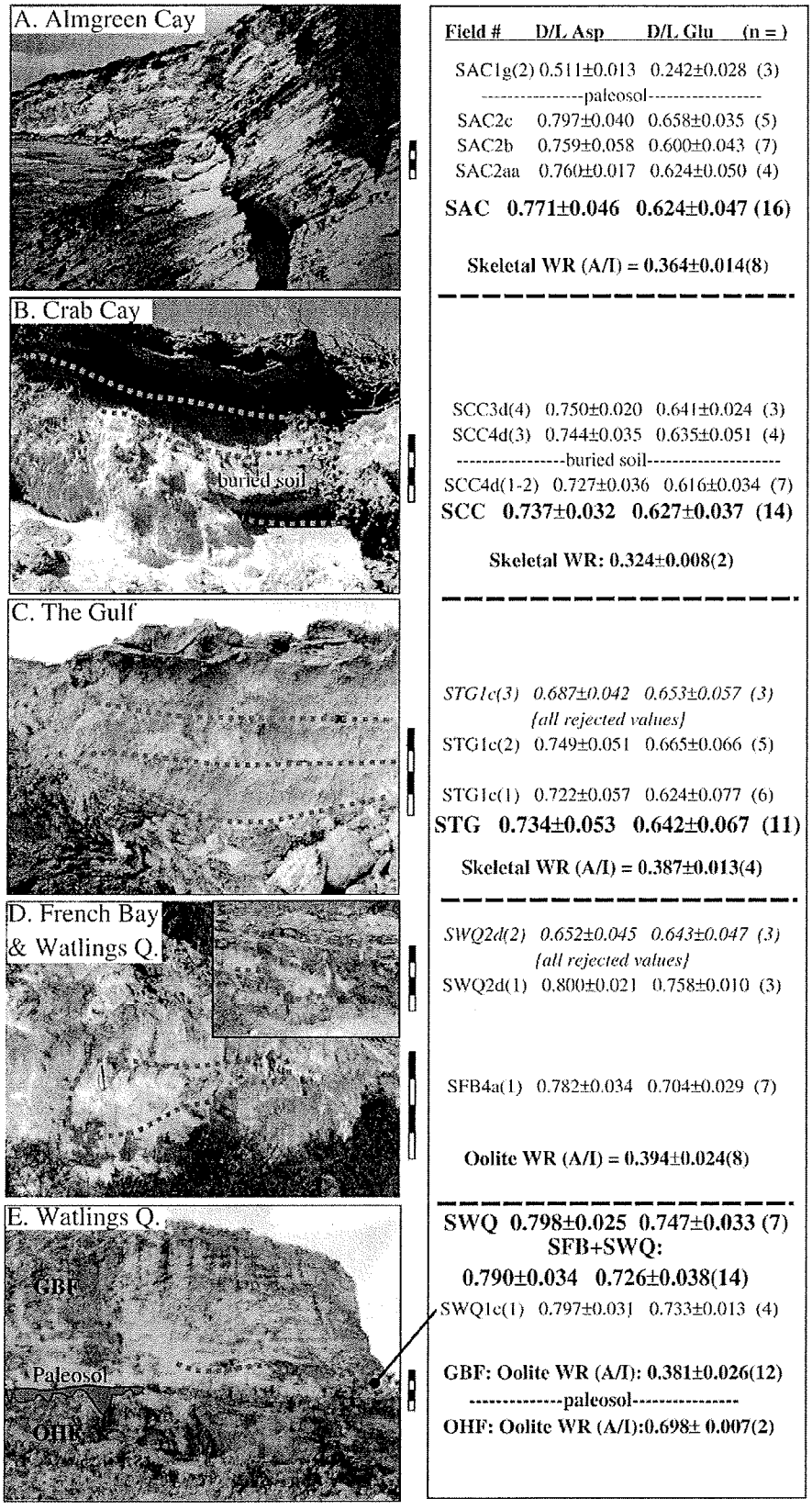

Fig. 7. Stratigraphy and AAR data from Pleistocene soil sequences. Stratigraphic names are provided in Table 1 and A–E site panels located in bold lettering in Fig. 2. Bold numbers are site aggregate mean values. WR = whole-rock samples. Scale bars are 1 m.

D/L to a power of 1.6, we obtained the highest r^2 value with sample age, yielding the linear relation:

$$y = 13104(D/L)^{1.6} - 108 (r^2 = 0.950;\ n = 23)$$

where y = age in cal BP.

For Glu, the rate of racemization over the past 7000 years is linear, and the calibrated age equation is:

$$y = 19238(D/L) - 345 (r^2 = 0.935;\ n = 23)$$

The age models assume that the ^{14}C ages are accurate. The scatter in the D/L versus ^{14}C age relation may reflect a variable dead carbon effect, although this effect is probably relatively small given that most dated shells were collected from mid and late Holocene dunes, and therefore the age difference between the shell and the substrate is expected to be small. Variable surface-heating effects could possibly influence the rate of racemization as well. These effects may combine or offset each other with the ultimate effect of "time averaging" the variability inherent in both ^{14}C and amino acid geochronology, yielding the reasonably consistent relationship observed between D/L and ^{14}C age. These equations can be used to estimate ages from D/L values for well-preserved *Cerion* from the sites on San Salvador Island. Like Kosnik et al. (2008), we recommend that the mean of the inferred ages from the two amino acids, Asp and Glu, be used as the preferred "AAR age" (Appendix A). The overall uncertainty associated with the age estimates based on these equations is probably ≤100 yr over the last millennium and ≤500 yr over the last 7 ka. (see Hearty and Kaufman in review for discussion).

3. Chronostratigraphic results

3.1. Whole-rock A/I aminostratigraphy

The resulting whole-rock A/I aminostratigraphy for SSI is consistent with the field-derived lithostratigraphic succession of Hearty and Kindler (1993) as well as the regional whole-rock A/I aminostratigraphy of Hearty and Kaufman (2000) (Table 3). Several formations and member subdivisions are discernable based on morphostratigraphy and mean whole-rock A/I values (Table 3).

The peak last interglacial (MIS 5e) is characterized by several distinct eolianite ridges that extend continuously over several kilometers (Figs. 2 and 3). The onset of MIS 5e is represented by at least four large concave or 'catenary' beach ridges (cf., Garrett and

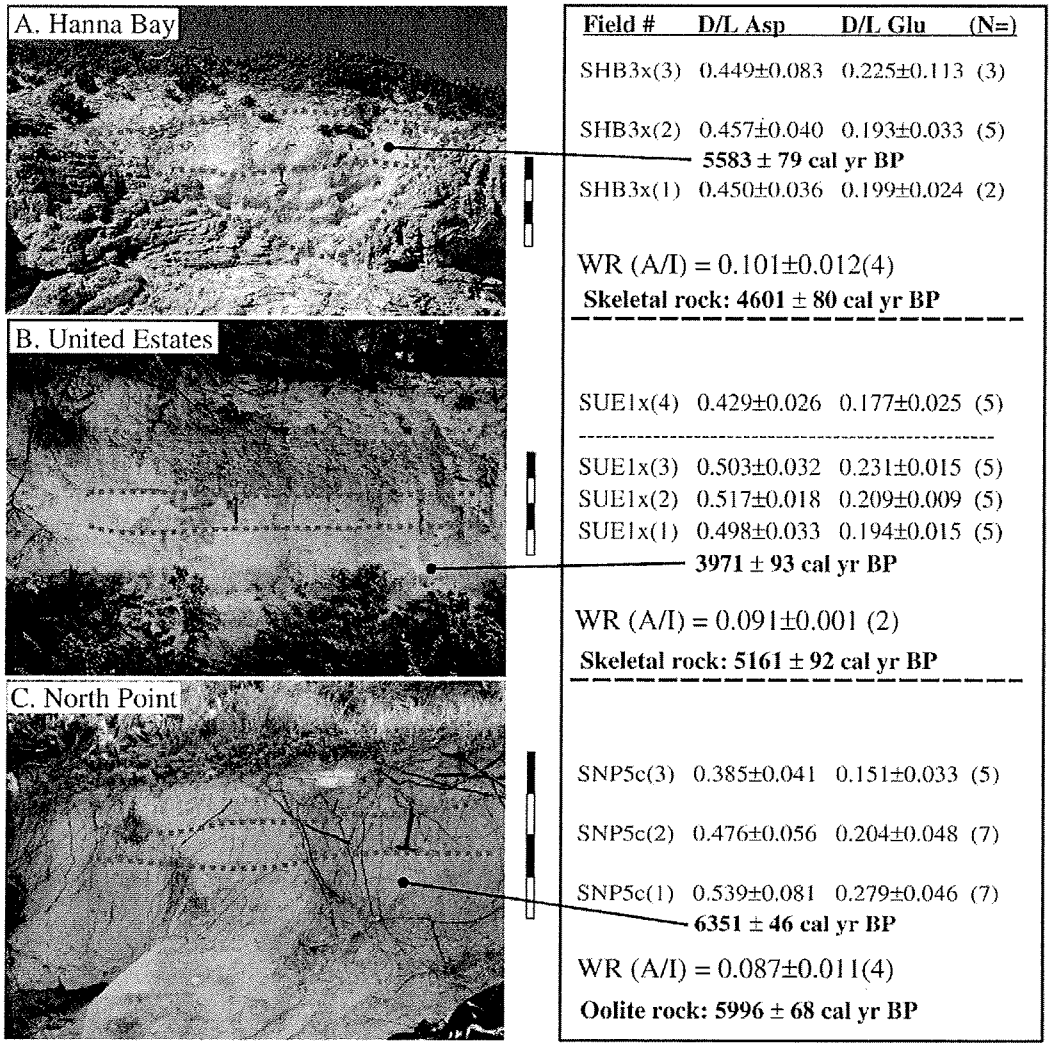

Fig. 8. Stratigraphy, AAR, and AMS ^{14}C data from Holocene soil sequences. Stratigraphic names are available in Table 1 and A–C panels located in Fig. 2. Bold numbers are site aggregate mean values. WR = whole-rock samples. Scale bars are 1 m.

Gould, 1984) over 40 m high deep within the interior of SSI (i.e., circled phases 1 and 2 of Substage 5e oolite in Fig. 2). Two samples (each comprising 2 subsamples) from Observation Tower Road (SOT on Figs. 2 and 3) yield an average A/I of 0.462±0.020 (n=2). These values compare to a mean of 0.377±0.030 (n=12) for the more seaward younger ridges of MIS 5e at French Bay (Figs. 2 and 3). The younger Almgreen Cay Formation (MIS 5a) represents a brief, but voluminous accumulation of bioclastic sediment attributed to MIS 5a (Figs. 2 and 3); Hearty and Kindler, 1993). MIS 5a generally yields lower, though overlapping, A/I values (mean of 0.349±0.045; n=7) compared to MIS 5e. Elsewhere in the Bahamas (Table 3; Kindler and Hearty, 1996; Hearty and Kaufman, 2000), statistically distinct A/I values are common from stratigraphically equivalent sites. In terms of physical characteristics, MIS 5a is distinguished from the MIS 5e by its younger and bluff-like geomorphology, distinctive skeletal composition, and larger and wider *Cerion* shell forms (Hearty et al., 1993).

The glacial lowstands of MIS 4-2 are represented by reddish brown, clayey soils, while the interglacial highstand of MIS 1 (the Holocene) comprises multiple phases of eolian deposition defined by the Rice Bay Formation. Unfortunately, the dune sediments from Holocene deposits of both the oolitic North Point Member and the stratigraphically younger bioclastic Hanna Bay Member (Figs. 2 and 3) have indistinguishable mean values centered at A/I of 0.098±0.015 (n=4), perhaps due to the somewhat slower Ile epimerization rate in ooids compared to skeletal sediments.

3.2. *Cerion* D/L aminostratigraphy

3.2.1. *Screening of sample D/L data*

Each amino acid racemizes at a characteristic rate. Under ideal conditions, the extent of racemization for different amino acids covaries according to a predictable function (Fig. 5). Analyses by RPC yields D/L values for multiple amino acids, and results can be compared to assess their internal consistency. The covariance between D/L values in Glu and Asp has been used previously to identify outliers for studies based on molluscan shells (Laabs and Kaufman, 2003), ostracode valves (Kaufman, 2003), and foraminifera tests (Hearty et al., 2004; Kaufman, 2006). Kosnik and Kaufman (2008) suggested that specimens should be screened based on the extent to which the ages inferred using different amino acids agree, following the development of the age models. The age models are calibrated based on ^{14}C ages over the last 7 ka only (Table 4) and includes shells with Glu D/L values <0.4. We chose a screening cut-off of 0.4 ("Y value"; see Kosnik and Kaufman, 2008 for details), so that any subsample with ages inferred from Asp and Glu that differed by either more than 400 yr or by more than 40% was rejected (inferred ages of Holocene shells, and shells that were rejected are listed in Appendix A). To screen the results from Pleistocene shells, we simply extrapolated the age equations, but choose a broader cut-off (Y=0.5). Although not ideal, this procedure provides an objective means of identifying outliers relative to the trend defined by the rest of the group.

A total of 21 of the 150 *Cerion* D/L samples (14%) were rejected using this procedure (Fig. 5). The majority of these rejected samples (i.e., 16 of the 21) were from the Pleistocene sequence (n=81). Nearly all of the rejected samples had Glu D/L values that were *higher* than expected compared with the corresponding Asp D/L. Some of rejected shells can be attributed to the intentional collection of shallowly buried and leached samples. We collected these to assess the results from less-than-optimal shells, and for subsequent studies of shell morphometry and biostratigraphy. Many of the rejected shells correspond to the reversal of D/L values in shells that attained quasi-equilibrium D/L values of ~0.80 (Fig. 5), then decreased as amino acid concentrations decreased with sample age. A similar pattern of increasing then decreasing A/I values with decreasing amino acid concentration was recently documented for land snails and whole rock samples from Plio-Pleistocene beds in Western Australia (Hearty and O'Leary, 2008). If this progression applies to our dataset, it implies that, as D/L values decrease with sample age, the diagenetic attrition of D-Asp is more rapid than for D-Glu. In this case, most outliers in Fig. 5 originated in thin, glacial-age reddish-brown soils and in which most or all shells in the samples (e.g., Samples SFR1x, STG1c(3), and SWQ2d(2) in Fig. 6 and Appendix A) show signs of amino acid degradation, probably by preferential leaching (Roof, 1997).

The covariance of D/L Asp and Glu in the 129 retained *Cerion* samples was used to distinguish both major and minor units of the SSI stratigraphy (Table 1; Fig. 6), and demonstrates the range of intra-unit values between 140 ka and living shells on SSI. The racemization reaction is several times faster during the Holocene, and thereby more clearly discriminates the major subdivisions of North Point and Hanna Bay Members, as well as surface dead and living shells (Fig. 6). In the Pleistocene, shells from the type localities of the Almgreen Cay and Grotto Beach Formations are readily distinguished.

3.2.2. *D/L in Cerion from MIS 5e and MIS 5a: Pleistocene Grotto Beach and Almgreen Cay Formations*

Pleistocene units yield D/L Glu values consistent with early and late MIS 5 as defined by earlier lithostratigraphic and aminostratigraphic studies (Hearty and Kindler, 1993). Fourteeen *Cerion* of the MIS 5e (peak last interglacial) at the type locality of the French Bay Member and Watlings Quarry (Fig. 7DE) produce an aggregated mean D/L Asp

Table 5
Mean simple morphometric data from ranked sites from major stratigraphic subdivisions in SSI

Field #	Rank#	W	±1σ	H	±1σ	H/W	±1σ	$H+W$	±1σ	N
Holocene (cf. Rice Bay Fm)										
SCC1z live	4	11.40	0.34	26.98	1.81	2.37	0.12	38.38	2.06	12
SHB3z live	7	10.69	0.52	24.81	1.10	2.33	0.17	35.50	1.08	13
SHT1z	24	10.29	0.78	24.54	2.52	2.38	0.14	34.84	3.19	11
SFR1x	17	11.88	0.86	28.66	2.58	2.42	0.18	40.55	3.21	18
SNP5c(3)	31	10.37	0.81	24.09	1.80	2.33	0.12	34.46	2.50	9
SUE1x(4)	32	11.08	0.88	25.52	3.09	2.30	0.18	36.59	3.81	12
SHB3x(3)	33	10.55	0.50	24.03	1.64	2.28	0.16	34.58	1.85	14
SHB3x(2)	35	10.29	1.06	24.53	3.05	2.38	0.11	34.82	4.05	20
SUE1x(3)	36	10.59	0.89	26.05	2.50	2.46	0.16	36.64	3.22	20
SUE1x(2)	37	10.14	0.76	24.61	2.16	2.43	0.17	34.76	2.71	18
SUE1x(1)	38	10.10	0.97	25.23	2.03	2.51	0.27	35.33	2.52	12
SNP5c(2)	39	10.01	0.43	23.45	1.33	2.34	0.10	33.46	1.63	13
SHB3x(1)	41	9.30	0.71	23.25	3.89	2.49	0.23	32.55	4.60	2
SHB1x mid	42	9.80	0.28	22.90	0.99	2.34	0.17	32.70	0.71	2
SNP5c(1)	43	9.34	0.61	22.63	1.83	2.42	0.11	31.97	2.38	23
Late-Late Pleistocene (cf. Almgreen Cay Fm)										
SAC1g(2)	46	11.10	0.51	27.10	1.83	2.44	0.16	38.20	2.05	6
SCC3d(4)	49	11.73	0.41	24.91	2.04	2.12	0.18	36.64	2.15	9
SCC4d(3)	50	12.01	0.85	24.56	2.25	2.05	0.14	36.58	2.91	8
SCC4d(1-2)	51	12.11	0.57	25.04	0.94	2.07	0.09	37.14	1.32	16
SAC2c	56	11.18	1.11	24.38	1.40	2.19	0.14	35.56	2.37	5
SAC2b	58	11.18	0.56	23.61	1.73	2.12	0.17	34.79	1.92	9
SAC2aa	59	10.53	0.48	22.34	1.29	2.13	0.14	32.86	1.48	8
STG1c(3)	62	9.20	0.50	21.35	1.40	2.32	0.12	30.55	1.76	13
STG1c(2)	64	8.93	0.60	20.78	1.61	2.33	0.12	29.71	2.11	30
STG1c(1)	65	9.37	0.55	21.94	1.69	2.34	0.15	31.31	2.05	16
SMH1b	68	7.62	0.35	15.81	1.01	2.08	0.12	23.42	1.20	17
Late Pleistocene (cf. Grotto Beach Fm)										
SWQ2d(2)	71	9.62	0.50	20.77	1.48	2.16	0.15	30.39	1.75	9
SWQ2d(1)	73	8.68	0.77	17.82	1.20	2.06	0.11	26.50	1.87	5
SWQ1d(1)	72	9.79	0.59	20.74	1.10	2.12	0.14	30.54	1.41	14
SWQ1c(1)	79	9.19	0.49	19.51	1.17	2.13	0.13	28.70	1.45	7
SFB4b(1)	85	8.91	0.36	18.64	0.91	2.10	0.14	27.55	0.93	16

Field numbers explained in Fig. 1. Rank and associated D/L data from equivalent levels are available in Table 2. Individual shell morphometric measurements are plotted in Fig. 9A/B and in archive Appendix B along with raw RPC data.

and Glu of 0.790±0.034 and 0.726±0.038 (n=14), respectively. The morphostratigraphically younger MIS 5a deposits at the Almgreen Cay type locality and nearby Crab Cay (Fig. 7ED) produce equivalent D/L Asp and Glu aggregate means of 0.771±0.046 and 0.624±0.047 (n=16) (SAC) and 0.737±0.032 and 0.627±0.037 (n=14) (SCC), respectively. Note that D/L Asp from these younger deposits show little difference compared to the French Bay Member, indicating that this reaction is approaching equilibrium.

Lower, middle, and upper soils of MIS 5a show little difference in their mean Glu D/L, suggesting a short time interval between oldest and youngest *Cerion* samples, which is consistent with a rapid emplacement of this MIS 5a deposit. At both Almgreen and Crab Cays, thermal effects appear to have slightly, although not significantly, elevated the Glu D/L values of the uppermost levels (<1 m depth). Combined values of D/L Glu are marginally higher at The Gulf (Fig. 7C) with a mean of 0.642± 0.067 (n=11), perhaps indicating minor thermal effects. The low-lying

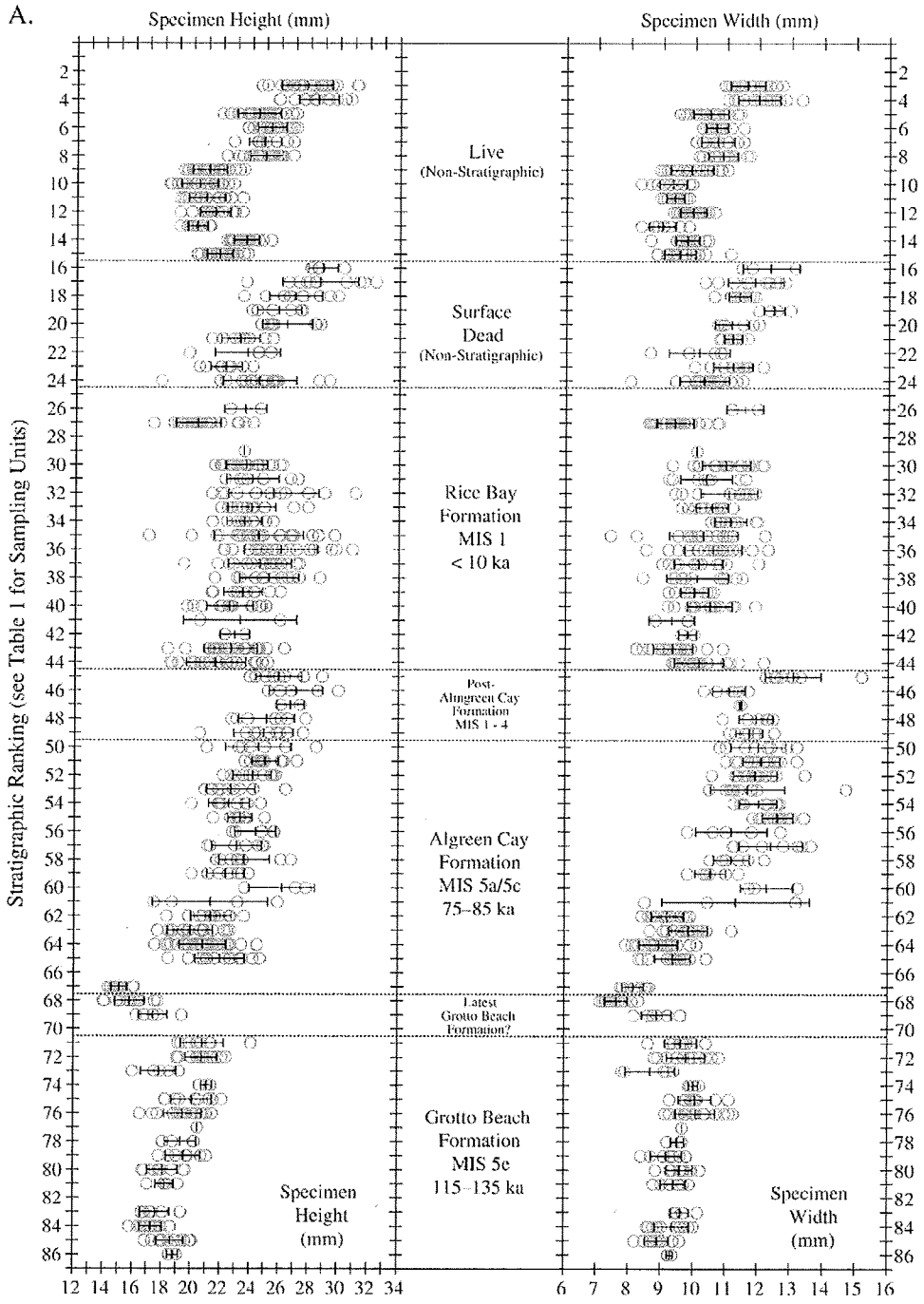

Fig. 9. A/B. Morphological changes in *Cerion* shells keyed to major units over past 140 ka. Height (H), width (W), H/W ratio, and size ($H+W$) are shown in the respective columns in the graph. Circle symbols in gray are individual shell measurements per collection; black bar represents mean and 1σ standard deviation. Stratigraphic rank is determined by 1) physical stratigraphic superposition (if known); 2) D/L Glu, then D/L Asp; and 3) whole-rock A/I of host rocks containing *Cerion*. Ranking does not apply to live and surface dead collections in which cases numbers are used for identification and tracking only.

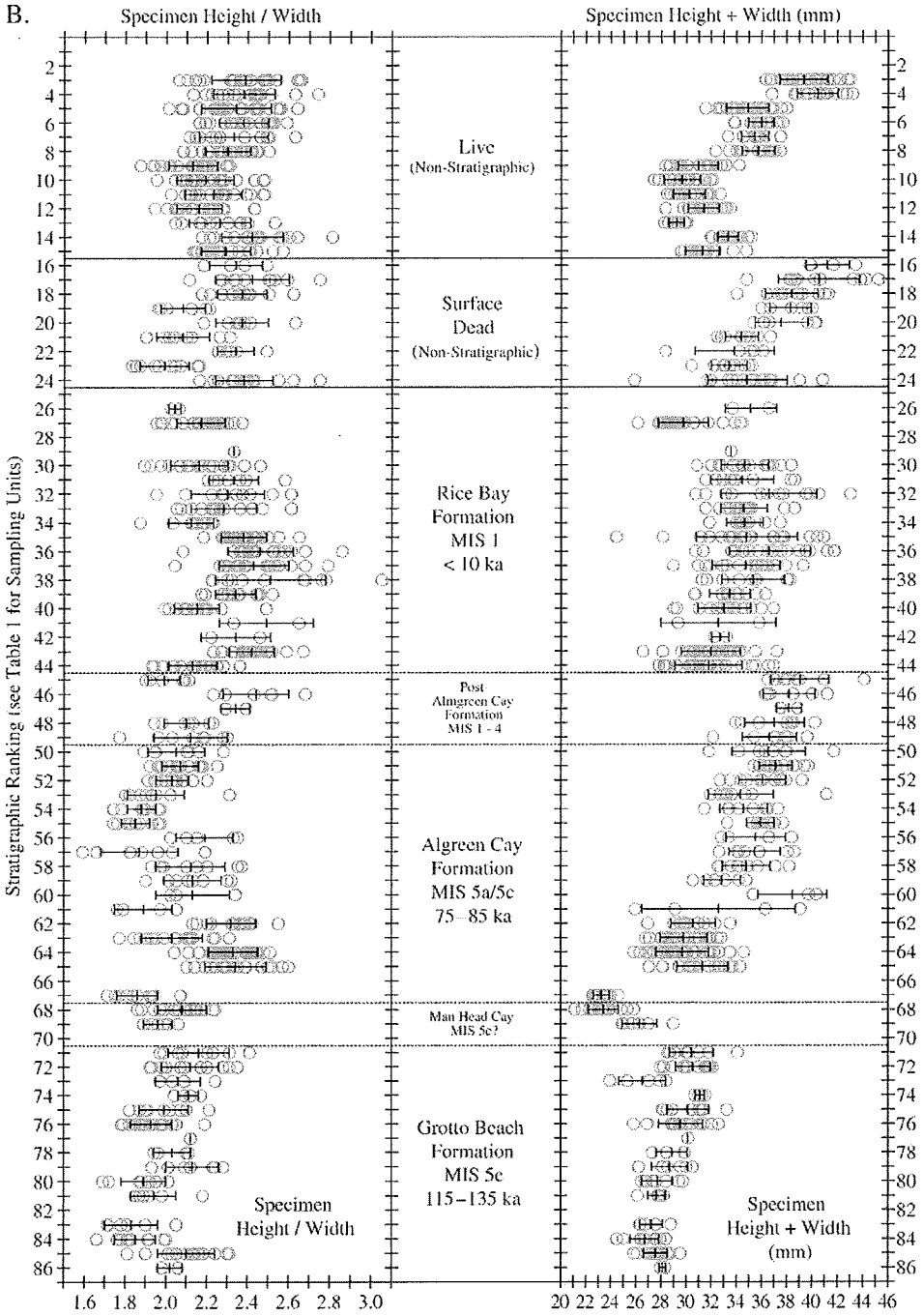

Fig. 9 *(continued).*

section on the exposed southern coast was also apparently subjected greater diagenetic alteration (e.g., leaching) in the upper unit, which produced only rejected values (Fig. 7C), perhaps due to shallow exposure and more frequent wetting by waves and sea spray. However, D/L Glu from the lowest and most protected unit in the section is precisely concordant with the type locality of the Almgreen Cay Formation at 0.624±0.077 (n=6). The overall mean D/L Glu values unambiguously support previous respective correlations with of Almgreen Cay and Grotto Beach Formations with MIS 5a and 5e (Hearty and Kindler, 1993, 1994; Hearty and Kaufman, 2000).

3.3. AMS ^{14}C data and application of the AAR age model

3.3.1. Comparison of AMS ^{14}C and AAR ages from Holocene (MIS 1) samples

Holocene sediment (n=3) and *Cerion* samples (n=5) were selected for AMS ^{14}C dating (Table 4) based on D/L ratios (Fig. 8). These AMS ^{14}C ages provide constraints on sediment formation age, emplacement and terrestrial colonization of dunes, and initiation of soil development. An AMS ^{14}C age from the type locality of the North Point Member (SNP5c(1); Table 1) oolite is 5996±68 cal BP (Table 4), while a

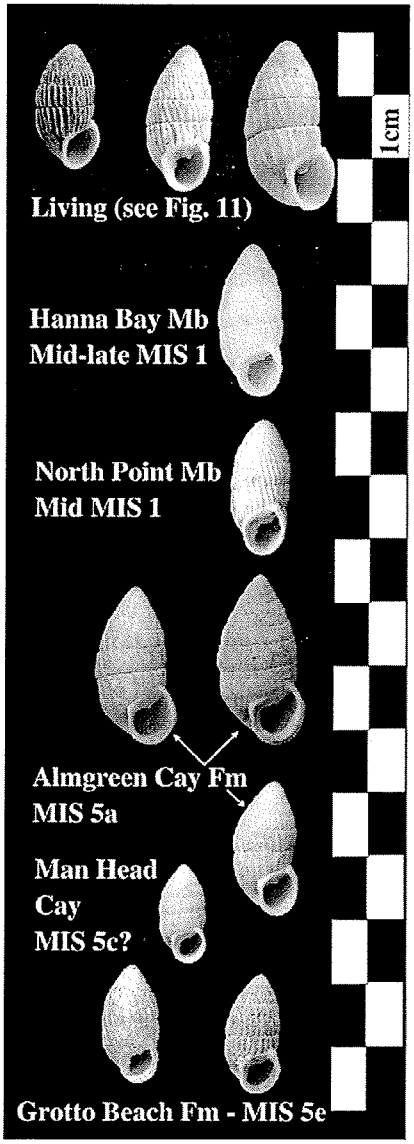

Fig. 10. Images of representative fossil and living shells of *Cerion* representing the stratigraphic succession of SSI (Table 1) over the past 140 ka.

skeletal dune from United Estates (SUE) produced an age of 5161±92 cal BP. The ^{14}C age of the type Hanna Bay Member (SHB) skeletal eolianite is 4601±80 cal BP (Fig. 8ABC). These calibrated dates mark the mean age of formation of the marine ooids and skeletal organisms comprising the dune sediments, and are considered to be reasonably accurate. The oldest *Cerion* shells, determined by RPC, from capping soils at each of these three localities (SNP, SUE, and SHB) yielded AMS ^{14}C ages of 6351±46, 3971±93, and 5583±79 cal BP, respectively (Fig. 8; Table 4).

The age structure of each of these deposits is revealed from average D/L Asp and Glu AAR ages of *Cerion* in soils overlying the three eolianites. AAR ages are calculated from equations above (results in Appendix A) provide some informative comparisons with ^{14}C ages. The same shell producing the 6351 cal BP age from SNP5c(1) produced a mean AAR age of 5868 yr. The age range of seven *Cerion* from the same level is 3200–5900, with a mean age of 4920±970 yr. At United Estates, the same shell producing the 3972 cal BP age produced a slightly older mean AAR age of 4217 yr. Five *Cerion* shells from SUE1x (1) yield a mean of 3790±360 yr. The results from these two cases suggest that the ^{14}C ages from *Cerion* are relatively accurate having only a minor age anomaly of a few hundred years to none at all. In the case of the Hanna Bay subunit SHB3x(2) (Fig. 8A), the same shell with a ^{14}C age of 5583±79 cal BP produced a significantly younger AAR age of 4083 yr, clearly suggesting a significant anomaly of 1500 yr. In contrast, the AAR age of five shells from this level of 3560±520 yr is compatible with the ^{14}C sediment age of 4600 yr, and is thus appears to be representative of the time of development of this soil horizon.

In summary, our data indicate the ooids at the type locality of the North Point Member formed in the sea around 6000 yr ago, were transported into an eolian facies, and then rapidly colonized by terrestrial organisms between about 5500 and 4500 yr ago. The skeletal sediment at the Hanna Bay type locality appears to have formed on the shelf around 4500 yr ago, and subsequently its dunes were also rapidly emplaced, vegetated and colonized between 4000 and 3000 yr ago. These whole-rock and *Cerion* ages in this study are older than previous conventional ^{14}C ages (Carew and Mylroie, 1987) on the same type localities by ~1000 (North Point Member) to ~2000 yr (Hanna Bay Member). These differences might be explained in part by the exclusion of cements from our whole-rock samples, which would tend to decrease the bulk sediment age, or perhaps inconsistencies in marine reservoir calculations.

3.3.2. Ages of younger dunes and surface dead shells

The oldest *Cerion* in weak soils on submodern dunes yielded, and a ^{14}C age of 865±67 cal BP at Holiday Track (SHT1z). The mean D/L Asp of 0.224 and D/L Glu of 0.058 are converted to an average AAR age of 930 yr. Another shell from the same deposit produced a mean AAR age of 961 yr, supporting a younger phase of dune emplacement and colonization on the windward east coast that post-dates the formation of the Hanna Bay Member (as in Hearty and Kindler, 1993).

Some surface dead samples show an unexpectedly high range of AAR ages (Table 5; Appendix A). For example, three surface dead shells from Crab Cay (SCC1z) range in AAR age from 370 to 3500 yr, while another site at Man Head Cay produced ages from 270 to 2280 yr. Some of the AAR ages are corroborated by independent ^{14}C ages (as at SHT1z above), but extensive surface heating, or possible reworking of fossil shells by hermit crabs (Walker and Hearty, 1993) should also be considered.

4. Trends and patterns of change in *Cerion* shell morphology

We assess the changes of the gross morphology of *Cerion* sample populations spanning the interval from MIS 6/5e transition to the present. Individual and mean *Cerion* shell measurements (*H*, *W*, *H/W*, and *H+W*) for 986 shells from 83 samples, are presented in Fig. 9A/B, Table 5, and Appendix B. The numerical ranking of samples is based on the combination of stratigraphic position and amino acid values presented above. The following correlations are established between MIS, major rock units, and numerical rankings (in parentheses): MIS 5e (#86-71); MIS 5a/c? (at Man Head Cay, #70-68); MIS 5a (#67-50); MIS 4-2 (#49-45); mid-MIS 1 (North Point Member) and late MIS 1 (Hanna Bay Member) (#44-25). Numerical rankings for surface dead (#24-16) and living shells (#15-3) are neither stratigraphic nor age-ranked, and stratigraphic ranking members are assigned solely for tracking and reporting purposes.

4.1. Interglacial enlargement and variability within formations

The most conspicuous temporal trend in SSI *Cerion* morphology is an overall increase in size during MIS 5e, MIS 5a, and MIS 1 (Fig. 9A). This observation is less pronounced during MIS 5e compared to MIS 5a and 1. As size increases, *H/W* also changes markedly (Fig. 9A), indicating that shells are not simply getting larger, but changing in their relative dimensions of height and width (Fig. 9B). In both MIS 5e and MIS 5a series, width increases while height remains relatively

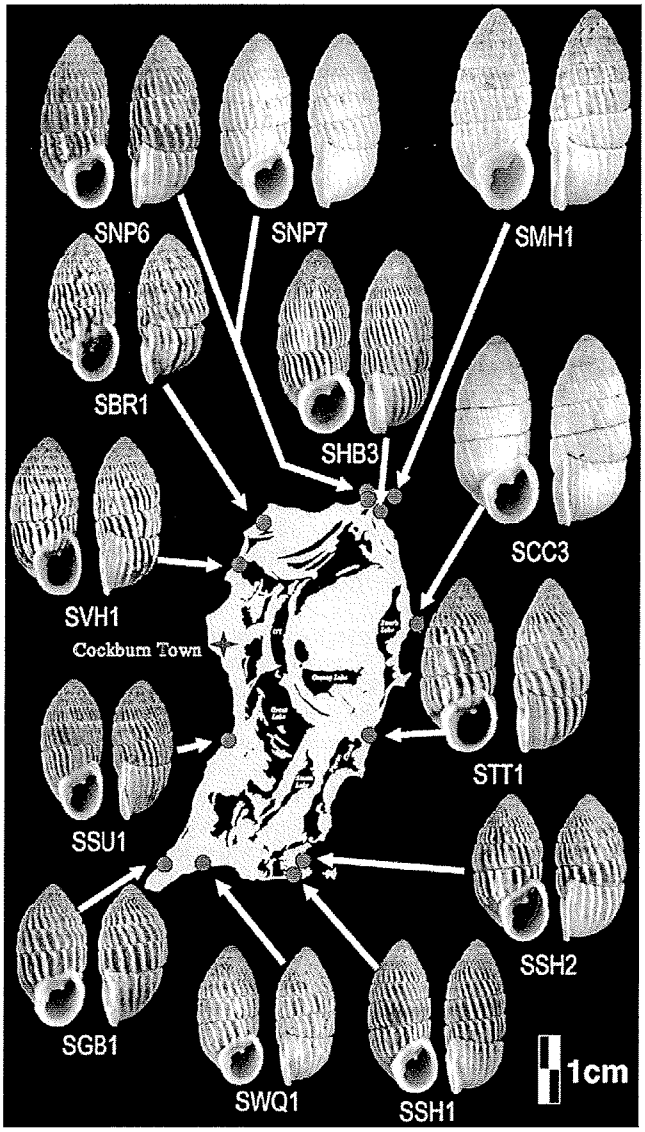

Fig. 11. Images of representative living shells collected from 13 locations of SSI.

stable early in the interglacial, while the opposite relationship (height changes greater than width) is the case later in the interval. Such trends are less apparent during the Holocene. Other than a few outliers, a marked deviation from this trend is a decrease in shell size during MIS 5c on Man Head Cay (SMH). In terms of overall trends in variability in shell morphology (i.e., the range of shells sizes within stratigraphic levels), MIS 5e clearly has the lowest, while MIS 5a is intermediate, and the Holocene and living levels have the highest variability (expressed as "±" in Table 5) of shell dimensions (Fig. 9).

4.2. Shell form during different interglacials

A comparison of size and shape, along with qualitative observations on shell color and ornamentation (following from Hearty et al., 1993), through each interglacial interval as well as sub-phases of the Holocene reveal a substantial diversity of forms (Fig. 10). Throughout their respective interglacials, MIS 5e shell forms appear nearly the same, whereas MIS 5a shell forms are changing with marked variability. However, as clear from Fig. 9, changes in size through most levels and ages are progressive. In general, MIS 5e shells are small, ribby and white or brown, show only a slight increase in size over MIS 5e, and remain extremely stable in appearance over the entire interglacial. Fossils from Man Head Cay are similar, but smaller, than MIS 5e shells. MIS 5a shells are highly variable in size, shape, color, and ornamentation within and between levels (ribby and smooth; dark and light, wide and narrow), but this variability generally decreases toward the end of the interval (Figs. 9 and 10). In the northeastern corner of the island, early to mid MIS 1 shells are small and ribby, and progressively increase in size and decrease in ribbiness up through living forms (Fig. 11).

4.3. Island-wide trends in living Cerion populations

Treatments of *Cerion* species on SSI have produced contradicting taxonomic views (Rose, 1989; Gould, 1997) and several informally described "species". As a result, in agreement with Baldini et al. (2007:174), we choose not to engage in species nomenclature as neither proof nor consensus exists with respect to species-level taxonomy, particularly as hybridisation appears to be a pervasive phenomenon. On SSI, living shells are variable in size, shape, ribbiness, and color in a SW–NE pattern across the island (Fig. 11). Southern and western shells (SSU, SGB, SWQ, SSH1/2) are smaller, more ribby, and darker, while northeastern forms are larger, less ribby and lighter (Fig. 11). Live shells from The Thumb (STT) appear to be hybrids between northeastern outer cays and southwest forms, as do those from Hanna Bay and North Point localities.

4.4. Apparent rates of change in shell form

If AAR age versus shell size is plotted for *Cerion* from the lower two sampled levels (SNP5c(1) and (2)) from the North Point Member, a relatively rapid increase in shell size is manifest over the interval from 6000 to 3000 yr (Fig. 12). During this interval, the general shell size increases by ~7 mm from ~33 to ~40 mm. The average rate of increase in shell size over this period is thus about 2–2.5 mm/kyr. Shell changes are most clearly documented in Holocene samples where racemization rates are rapid enough to distinguish centuries. If similar time intervals are assumed for Pleistocene interglacial soil sequences (a few

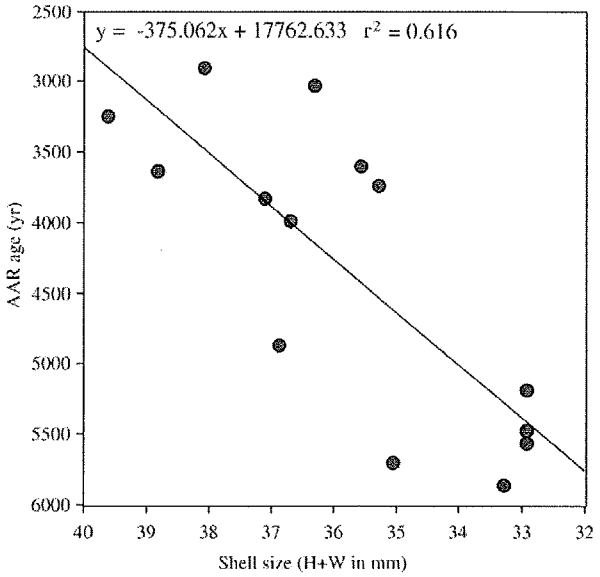

Fig. 12. Plot of AAR age versus total size (*H+W*) of *Cerion* shells from successive soil levels at North Point Member (SNP5c(1) and (2)), SSI (Plate C in Fig. 8) showing rate of change in individual shell size.

kyr), as we suspect for Crab Cay and The Gulf, it is reasonable to infer similarly rapid changes through these sequence.

5. Discussion

5.1. Geochronology

The whole-rock limestone aminostratigraphy (Hearty and Kindler, 1993; Hearty and Kaufman, 2000) is confirmed and further supported by the RPC *Cerion* aminostratigraphy based on D/L Asp and Glu. In particular, the Holocene lithostratigraphy and biostratigraphy are greatly refined, showing subdivisions in most soil sequences. AMS ^{14}C ages from MIS 1 oolite (North Point Member) and skeletal dunes (Hanna Bay Member) indicate the initial formation of sediments occurred sequentially on the shelf between ~6000 and ~4600 cal BP. These ages are older than previously reported (Carew and Mylroie, 1987). *Cerion* ^{14}C ages from the same stratigraphic sections are inverted (6351±46 and 5583±79 cal BP) by 350 to 1000 yr, which may reflect a dead carbon anomaly or time-averaging (i.e., physical reworking, hermit crab bioturbation, etc.; Kowalewski et al., 1998; Yanes et al., 2007). Regardless, it appears there was a rapid shelf-to-shore sediment flux and subsequent colonization of the new eolian substrate by plants and animals.

5.2. Morphological changes in Cerion over the past 140 ka

The stratigraphic and AAR age-ranking of shells in presumably bioturbated soil sequences reveals the persistent changes in shell morphology in 986 measured shells *Cerion* on SSI over 140 ka. However, change appears to be continuous and generally directional. In the broadest view of trends and patterns in *Cerion* shell morphology, shells have achieved greater net size over the past 140 ka. Under closer inspection of the biostratigraphy over three interglacial cycles, individual sites, and subunits representing over 30 time slices, consistent but more subtle trends are apparent.

Over ~10–15 ka of MIS 5e, shells become slightly larger, yet within very small limits of variability (Fig. 9). In contrast, at the onset of MIS 5a, shell change is extreme, expressing a very broad variability in form over perhaps a few thousand years. In only 2–5 ka of mid MIS 1, particularly in the northeast corner of SSI, shells increase in size within a moderate range of variability. The apparent stability in MIS 5e shell forms may be a reflection of stable climate or ecology. In contrast, we suggest the apparent instability of shell forms during MIS 5a may be the consequence of pronounced climate changes.

5.3. Possible underlying causes of change

Goodfriend (1986) reviewed various environmental factors that may influence shell size of various species, including moisture (wetter=larger shells), temperature (warmer=larger shells), and population density (greater density=smaller shells). Interglacials would likely be characterized by slightly warmer and wetter regional conditions, perhaps accounting for our observation of generally increasing shell sizes. With high sea level, small land-masses or islets may become isolated leading to higher density populations, and thus smaller shells, as exemplified by an extreme example at Man Head Cay.

Kemp and Bertness (1984) established from studies of *Littorina littorea* that shell shape is a function of growth rates related to diet, such that rapidly growing shells develop thin, globose shells, while slow growth results in thicker, taller shells. Our results show that in at least the MIS 5e and MIS 5a, width increases faster than height early in interglacials, with the opposite occurring later in the interglacial (Fig. 9). This pattern hints that early interglacials may provide a richer diet, resulting in faster growing, more globose shells.

5.4. Sea level and biogeographic changes

Most of SSI (~80%) currently exposes surficial geology that formed during MIS 5e (Fig. 1). Early in this interglacial substage, much of the island was submerged except for older middle Pleistocene hills which provided refugia for terrestrial fauna and flora (Hearty and Kindler, 1993; Hearty et al., 1993). Sediments were likely formed quickly on the productive shallow platform, and transported inland forming shore ridges and dunes, which in turn were quickly colonized by plants and animals. This new landscape and its presumably lush vegetation provided an expanded habitat of potentially greater niches for the previously isolated *Cerion* populations. Island growth continued during MIS 5e to nearly its present form. With MIS 5d sea-level regression, SSI reached its maximal land area of about 30% larger than present, but may have experienced a relatively temperate and moist climate for the next ~30 kyr. With the MIS 5a transgression reaching near present sea level (Vacher and Hearty, 1989), some lowland areas were flooded, and large dune bluffs were rapidly built up along the eastern shore. Snails colonizing these bluffs were much larger and globose than those of MIS 5e. The glacial periods to follow (MIS 4-2) preserved only a scant record of fossil snails, but the inference is that they became smaller during the glacials, as they appeared so in the NW corner of SSI during the earliest MIS 1 of MIS 1 at ~6500 cal BP.

5.5. Living Cerion on SSI: progenitors to progeny?

One to three living *Cerion* species have been suggested for SSI, but never formally described (Rose, 1989; Gould, 1997). Among 13 living circum-island samples collected for this study, an spectrum of hybrid forms exist between two apparent end-member forms (i.e., small, dark, ribby versus large, white, smoother). Our chronostratigraphic study documents that sample populations of fossil *Cerion* show marked and repeated morphologic patterns through the last ~140 kyr. In the absence of a chronostratigraphy, individual shells and some fossil sample populations might well be perceived as distinct species among the living forms (Fig. 10). However, our data reveal gradients of morphological change between such end-members.

Multiple *Cerion* extinctions and recolonizations during the 140 kyr record are deemed improbable given the relatively rich and continuous record. Hybridization appears evident among living populations on SSI, and is a recurrent theme in numerous studies (Mayr and Rosen, 1956; Woodruff and Gould, 1980; Gould and Woodruff, 1986; Goodfriend and Gould, 1996). Thus, based on these observations, we hypothesize that multiple species on SSI are unlikely, except perhaps in the modern record through human introductions. Most importantly, in all 80 levels examined, including living populations, despite displaying many diverse individual shell forms, *Cerion* sample populations appear consistently unimodal in their size, shape, and appearance, suggesting wide variation and flexibility within one biological entity (i.e., species) through time and space. Future DNA-based studies may clarify this issue.

Given that observed changes in shell form are continuous, cyclical, and generally directional, and that no single stratigraphic level contains multiple morphotypes, we propose that SSI was most likely occupied since the beginning of MIS 5e by a single, highly ecophenotypic lineage capable of producing a diversity of shell forms in response to short-term isolation and changing environmental pressures including predation. This and other working hypotheses will be rigorously examined in this age framework in future biostratigraphic, biogeographic, and morphometric studies.

6. Conclusions

Litho-, bio-, and aminostratigraphic data for San Salvador Island presented in previous and this present studies have established a chronostratigraphy for rocks and fossils over the past 140 ka. Relative

age ranking is possible across the study interval, and age resolution increases substantially during the Holocene. As the duration of glacial periods are represented by only a few shells in centimetres of reddened soil and atmospheric dust, our focus, by default, is on the period at the onset, duration, and cessation of interglacial periods.

AMS ^{14}C ages and over 150 RPC amino acid analyses from deposits of three successive interglacial sea-level cycles provide a means to examine morphological change in *Cerion*. Individual shells are age-ranked in a high-resolution time frame during the Holocene, while application of the age model of Hearty and Kaufman (in review) reveals the age structure of key deposits and type localities. The magnitude of potential age anomalies in ^{14}C ages on *Cerion* may be directly evaluated with AAR ages. RPC provides accurate age-sequencing of individuals or groups of fossils for biostratigraphic or phylogenetic studies throughout the late Pleistocene and Holocene.

Simple morphometric measures on 986 *Cerion* shells, when placed in a time-succession by stratigraphic and age criteria, demonstrate continuous and directional morphological changes on island-wide to intra-unit scales. The period of greatest rate of change coincides with the onset of interglacials, when the effects of sea level and environmental changes are most pronounced. Shell size increases only slightly and shape remains relatively stable through most of MIS 5e. In contrast, shell changes in early MIS 5a are characterized by pronounced inter-unit variations in size, shape, and ornamentation (Hearty et al., 1993).

In a single subunit of the Holocene North Point Member, *Cerion* shells incrementally increase in total size ($H+W$) by about 25% in 3 ka. Similar rates of change are estimated for Pleistocene soil sequences. In the tradition of *Cerion* taxonomy, if individual shells from isolated fossil levels were viewed independently of this biostratigraphy (Fig. 10), it is probable that additional *Cerion* species would be named. However, we observe gradients of intermediate sizes and shapes, demonstrating that change is progressive and reversible, likely reflecting changes in ambient environment and ecological conditions. Ecophenotypy is a favoured mechanism to explain the observed temporal changes in *Cerion* shell form over the past 140 ka. This evolutionary mechanism will be considered among other working hypotheses in future studies.

Acknowledgements

This research was supported by NSF award EAR 0106936 (Goodfriend, Gould, and Harasewych) by means of a subcontract to PJH. We greatly appreciate the involvement of J. Harasewych and his significant contributions to earlier versions of the manuscript. Thorough reviews of P. Kindler (U. Geneva) and an anonymous reviewer were insightful and constructive. We also thank the Bahamas Ministry of Agriculture and the Gerace Research Centre on SSI for their support. The Riding Rock Inn offered reduced rates in support of this project, while costs for AAR and AMS ^{14}C determinations were partially defrayed under a NSF Facility Grant numbers EAR-0620455 and EAR-0622235 to D. Kaufman (Northern Arizona U.) and T. Jull (U. Arizona), respectively.

Appendices A and B. Supplementary data

Supplementary data associated with this article can be found, in the online version, at doi:10.1016/j.palaeo.2008.06.003.

References

Baldini, L.M., Walker, S.E., Railsback, B., Baldini, J.U.L., Crowe, D.E., 2007. Isotopic ecology of the modern land snail *Cerion*, San Salvador, Bahamas: preliminary advances toward establishing a low-latitude island paleoenvironmental proxy. Palaios 22, 174–187.

Carew, J.L., Mylroie, J.E., 1985. The Pleistocene and Holocene stratigraphy of San Salvador Island, Bahamas, with reference to marine and terrestrial lithofacies at French Bay. In: Curran, H.A. (Ed.), Pleistocene and Holocene carbonate environments on San Salvador Island, Bahamas: 1985 Annual Meeting Geological Society of America Field Guide. Geological Society of America, Orlando, FL, pp. 11–61.

Carew, J.L., Mylroie, J.E., 1987. A refined geochronology for San Salvador Island, Bahamas. In: Curran, H.A. (Ed.), Proceedings of the 3rd Symposium on the geology of the Bahamas: CCFL Bahamian Field Station, pp. 35–44.

Carew, J.L., Mylroie, J.E., 1995. Quaternary tectonic stability of the Bahamian archipelago: evidence from fossil coral reefs and flank margin caves. Quaternary Science Reviews 14, 145–153.

Clench, W.J., 1957. A catalogue of the Cerionidae (Mollusca: Pulmonata). Bulletin of the Museum of Comparative Zoology 116, 121–169.

Dall, W.H., 1905. Fossils of the Bahama Islands, with a list of the non-marine mollusks. In: Shattuck, G.B. (Ed.), The Bahama Islands. The Geographical Society of Baltimore, pp. 23–47. pls. 11–13.

Garrett, P., Gould, S.J., 1984. Geology of New Providence Island, Bahamas. Geological Society of America Bulletin 95, 209–220.

Goodfriend, G.A., 1986. Variation in land-snail shell form and size and its causes: a review. Systematic Zoology 35 (2), 204–223.

Goodfriend, G.A., Gould, S.J., 1996. Paleontology and chronology of two evolutionary transitions by hybridization in the Bahamian land snail *Cerion*. Science 274, 1894–1897.

Goodfriend, G.A., Stipp, 1983. Limestone and the problem of radiocarbon dating of land-snail shell carbonate. Geology 11, 575–577.

Gould, S.J., 1988. Prolonged stability in local populations of *Cerion agassizi* (Pleistocene–recent) on Great Bahama Bank. Paleobiology 14, 1–18.

Gould, S.J., 1997. The taxonomy and geographic variation of *Cerion* on San Salvador (Bahama Islands). In: Carew, J.L. (Ed.), Proceedings of the 8th Symposium on the Geology of the Bahamas and other Carbonate Regions. Bahamian Field Station, pp. 73–91. San Salvador, Bahamas.

Gould, S.J., Woodruff, D.S., 1986. Evolution and systematics of *Cerion* (Mollusca: Pulmonata) on New Providence Island: a radical revision. Bulletin of the American Museum of Natural History 182, 389–490.

Gould, S.J., Woodruff, D.S., 1978. Natural history of *Cerion*. VIII. Little Bahama Bank—a revision based on genetics, morphometrics, and geographic distribution. Bulletin of the Museum of Comparative Zoology 148, 371–415.

Hare, P.E., Mitterer, R.M., 1967. Non-protein amino acids in fossil shells. Carnegie Institution of Washington Yearbook 65, 236–364.

Hearty, P.J., 1998. The geology of Eleuthera Island, Bahamas: a Rosetta Stone of Quaternary stratigraphy and sea-level history. Quaternary Science Reviews 17, 333–355.

Hearty, P.J., 2002. A revision of the late Pleistocene stratigraphy of Bermuda. Sedimentary Geology 153 (1–2), 1–21.

Hearty, P.J., Kindler, P., 1993. New perspectives on Bahamian geology: San Salvador Island, Bahamas. Journal of Coastal Research 9, 577–594.

Hearty, P.J., Kindler, P., 1994. Straw men, Glass Houses, Apples and Oranges: a response to Carew and Mylorie's Comment on Hearty and Kindler, 1993. Journal of Coastal Research 10, 1095–1105.

Hearty, P.J., Kaufman, D.S., 2000. Whole-Rock Aminostratigraphy and Quaternary Sea-Level History of the Bahamas. Quaternary Research 54, 163–173.

Hearty, P.J., O'Leary, M.J., 2008. Carbonate eolianites, quartz sands, sea-level cycles, Western Australia. Quaternary Geochronology 3, 26–55.

Hearty, P.J., Kaufman, D.S., (in press). Chronostratigraphy for the central Bahama Islands based on ^{14}C ages and amino acid racemization in whole-rock sediment and *Cerion* land snails. Quaternary Geochronology.

Hearty, P.J., Miller, G.H., Stearns, C., Szabo, B.J., 1986. Aminostratigraphy of Quaternary shorelines around the Mediterranean basin. Geological Society of America Bulletin 97, 850–858.

Hearty, P.J., Vacher, H.L., Mitterer, R.M., 1992. Aminostratigraphy of Pleistocene limestones of Bermuda. Geological Society of America Bulletin 104, 471–480.

Hearty, P.J., Kindler, P., Schellenberg, S., 1993. A synthesis of the surficial geology of San Salvador Island, Bahamas. In: White, B., Curran (Eds.), Proceedings of the 6th Symposium on the Geology of the Bahamas, pp. 205–222.

Hearty, P.J., O'Leary, M.J., Kaufman, D.S., Page, M., Bright, J., 2004. Amino acid geochronology of individual foraminifer (*Pulleniatina obliquiloculata*) tests, north Queensland margin, Australia: a new approach to correlating and dating Quaternary tropical marine sediment cores. Paleoceanography 19, PA4022. doi:10.1029/2004PA001059.

Hearty, P.J., O'Leary, M.J., Donald, A., Lachlan, T., 2006. The enigma of 3400 cal BP coastal oolites in Tropical northwest Western Australia...why then, why there? Sedimentary Geology 186, 171–185.

Kaufman, D.S., 2003. Amino acid paleothermometry of Quaternary ostracodes from the Bonneville Basin, Utah. Quaternary Science Reviews 22, 899–914.

Kaufman, D.S., 2006. Temperature sensitivity of aspartic and glutamic acid racemization in the foraminifera *Pulleniatina*. Quaternary Geochronology 1, 188–207.

Kaufman, D.S., Manley, W.F., 1998. A new procedure for determining enta1omeric (D/L) amino acid ratios in fossil using reverse phase liquid chromatography. Quaternary Science Reviews 17, 987–1000.

Kemp, P., Bertness, M.D., 1984. Snail shape and growth rates: evidence for plastic shell allometry in *Littorina littorea*. Proceedings of the National Academy of Sciences 81, 811–813.

Kindler, P., Hearty, P.J., 1996. Carbonate petrology as an indicator of climate and sea-level changes: new data from Bahamian Quaternary units. Sedimentology 43, 381–399.

Kosnik, M.A., Kaufman, D.S., 2008. Identifying outliers and assessing the accuracy of amino acid racemization measurements for geochronology: II. Data screening. Quaternary Geochronology 3, 328–341.

Kosnik, M.A., Kaufman, D.S., Quan, H., 2008. Identifying outliers and assessing the accuracy of amino acid racemization measurements for geochronology: I. Age calibration curves. Quaternary Geochronology 3, 308–327.

Kowalewski, M., Goodfriend, G.A., Flessa, K.W., 1998. High-resolution estimates of temporal mixing within shell beds: the evils and virtues of time-averaging. Paleobiology 24, 287–304.
Laabs, B.J.C., Kaufman, D.S., 2003. Quaternary highstands in Bear Lake Valley, Utah and Idaho. Geological Society of America Bulletin 115, 463–478.
Maynard, C.J., 1913. Description of some species of the family Cerionidae. Appendix to vol. 5. Records of Walks and Talks with Nature, pp. 177–200. West Newton, MA.
Mayr, E., Rosen, C.B., 1956. Geographic variation and hybridization in populations of Bahama snails (*Cerion*). American Museum Novita 1806.
Miller, G.H., Brigham-Grette, J., 1989. Amino acid geochronology: resolution and precision in carbonate fossils. Quaternary International 1, 111–128.
Pilsbry, H.A., 1902. Family Cerionidae. Manual of Conchology, Second Series, Pulmonata, Vol. 14. Academy of Natural Sciences of Philadelphia 174–281.
Quensen III, J.F., Woodruff, D.S., 1997. Associations between shell morphology and land crab predation in the land snail *Cerion*. Functional Ecology 11, 464–471.
Reimer, P.J., Baillie, M.G.L., Bard, E., Bayliss, A., Beck, J.W., Bertrand, C., Blackwell, P.G., Buck, C.E., Burr, G., Cutler, K.B., Damon, P.E., Edwards, R.L., Fairbanks, R.G., Friedrich, M., Guilderson, T.P., Hughen, K.A., Kromer, B., McCormac, F.G., Manning, S., Bronk Ramsey, C., Reimer, R.W., Remmele, S., Southon, J.R., Stuiver, M., Talamo, S., Taylor, F.W., van der Plicht, J., Weyhenmeyer, C.E., 2004. INTCAL04 terrestrial radiocarbon age calibration, 0–26 cal kyr BP. Radiocarbon 46, 1029–1058.
Roof, S., 1997. Comparison of isoleucine epimerisation and leaching potential in the molluscan genera *Astarte*, *Macoma*, and *Mya*. Geochemica et Cosmochimica Acta 61 (24), 5325–5333.
Rose, J.A., , 1989. *Cerion* on San Salvador, Bahamas: Ecology and intraspecific variation. Unpublished Ph.D. dissertation, Harvard University, Cambridge MA, 9, 138 pp.
Rutter, N.W., Blackwell, B., 1995. Amino acid racemization dating. Geological Association of Canada. Geotext 2, 125–167.
Stuiver, M., Reimer, P.J., Reimer, R.W., 2005. CALIB 5.0. [web program and documentation].
Vacher, H.L., Hearty, P.J., 1989. History of Stage 5 sea level in Bermuda: review with new evidence of a rise to present sea level during Substage 5a. Quaternary Science Reviews 8, 159–168.
Walker, S.E., 1994. Biotic Interactions: Implications for *Cerion* biostratigraphy. The 7th Symposium of the Geology of the Bahamas, Abstracts with Programs, vol. 20.
Walker, S.E., Hearty, P.J., 1993. Do biotic interactions affect *Cerion*-based stratigraphy in the Bahamas? Geological Society of America Annual Meeting Abstracts with Programs, vol. 25, p. A52.
Woodruff, D.S., Gould, S.J., 1980. Geographic differentiation and speciation in *Cerion* — a preliminary discussion of patterns and processes. Biological Journal of the Linnean Society 14, 389–416.
Yanes, Y., Kowalewski, M., Ortiz, J.E., Castillo, C., Torres, T., de la Nuez, J., 2007. Scale and structure of time-averaging (age mixing) in terrestrial gastropod assemblages from Quaternary eolian deposits of the eastern Canary Islands. Palaeogeography, Palaeoclimatology, Palaeoecology 251, 79–85.